Biofabrication

TOPICAL REVIEW

Engineered assistive materials for 3D bioprinting: support baths and sacrificial inks

Lucia G Brunel[1,3], Sarah M Hull[1,3] and Sarah C Heilshorn[2,*]

[1] Department of Chemical Engineering, Stanford University, Stanford, CA, United States of America
[2] Department of Materials Science and Engineering, Stanford University, Stanford, CA, United States of America
[3] These authors contributed equally to this work.
[*] Author to whom any correspondence should be addressed.

E-mail: heilshorn@stanford.edu

RECEIVED
26 January 2022

REVISED
26 April 2022

ACCEPTED FOR PUBLICATION
29 April 2022

PUBLISHED
19 May 2022

Keywords: bioprinting, assistive material, support bath, sacrificial ink, biofabrication, hydrogel, tissue engineering

Abstract

Three-dimensional (3D) bioprinting is a promising technique for spatially patterning cells and materials into constructs that mimic native tissues and organs. However, a trade-off exists between printability and biological function, where weak materials are typically more suited for 3D cell culture but exhibit poor shape fidelity when printed in air. Recently, a new class of assistive materials has emerged to overcome this limitation and enable fabrication of more complex, biologically relevant geometries, even when using soft materials as bioinks. These materials include support baths, which bioinks are printed into, and sacrificial inks, which are printed themselves and then later removed. Support baths are commonly yield-stress materials that provide physical confinement during the printing process to improve resolution and shape fidelity. Sacrificial inks have primarily been used to create void spaces and pattern perfusable networks, but they can also be combined directly with the bioink to change its mechanical properties for improved printability or increased porosity. Here, we outline the advantages of using such assistive materials in 3D bioprinting, define their material property requirements, and offer case study examples of how these materials are used in practice. Finally, we discuss the remaining challenges and future opportunities in the development of assistive materials that will propel the bioprinting field forward toward creating full-scale, biomimetic tissues and organs.

1. Introduction

Over the past two decades, three-dimensional (3D) bioprinting has emerged as a promising additive manufacturing technique to pattern living biological materials into tissue-like constructs with unprecedented spatial precision [1]. In both the popular media and scientific literature, 3D bioprinting is often touted as a revolutionary technology that will transform the tissue engineering landscape. Specifically, 3D bioprinting has the potential to address an unmet need to closely recapitulate the structural complexity and biological function of human tissues. The long-term vision for 3D bioprinting involves the creation of *in vitro* mimics of human tissues with improved physiological relevance to humans over two-dimensional cell cultures or animal models, and the fabrication of functional tissue or organ replacements to address the critical shortage of donor organs for patients in need of transplants [2]. To this end, several types of 3D bioprinting technologies—including extrusion, stereolithography, inkjet, and laser-assisted printing—have been adopted [3]. The most widely-used 3D bioprinting approach for tissue engineering applications is extrusion-based bioprinting, in which a bioink—defined as a formulation of cells often in a composite with acellular material components [4, 5]—is loaded into a syringe and extruded in a pre-specified, layer-by-layer pattern to build the 3D construct [6]. Since bioinks by definition contain encapsulated cells, 3D bioprinting allows for fabrication of constructs with physiologic cell volume fractions (ranging from 1% to 2% in cartilage [7, 8] up to 90% in muscle [9–12]), which

would otherwise be challenging to achieve by seeding cells atop acellular 3D printed scaffolds. Despite the popularity of extrusion-based 3D bioprinting and growth in annual research output and commercialization [13], examples of bioprints with both form and function similar to native human tissues remain minimal, indicating that significant advancements in the field are still required.

The full potential of 3D bioprinting has yet to be realized in large part due to trade-offs between ease of fabrication and biomimicry of the printed bioinks. Born from the field of 3D printing (patented in the mid- to late-1980s [14–17]), early demonstrations of 3D printing with viable cells (patented in the early 2000s [18–20]) primarily used materials optimized for printability. Here, we define printability as the ability of a material to be extruded into continuous filaments that maintain their shape fidelity [21]. These bioinks are typically viscous and polymer-rich to retain high structural fidelity during and after printing. Because of the emphasis on printability, however, these materials often do not facilitate high levels of biological functionality due to suboptimal mechanical and biochemical properties for cells encapsulated within the bioink [5, 22]. On the other hand, for improved biomimicry, bioinks are often designed with consideration for tissue-specific endogenous material properties. While these materials are more conducive to maturation into tissue-like constructs, they are often ill-suited for 3D bioprinting due to their poor extrudability and/or weak mechanical properties. In particular, the susceptibility of these bioinks to collapse when printed in air limits the achievable scale and structural features of the print [23]. Furthermore, the size of bioprinted constructs is restricted by the need of encapsulated cells to have ready access to oxygen and nutrients [24]. Altogether, the trade-offs between achievable geometric complexity and biological functionality of bioinks remain a key challenge in printing tissue-like constructs.

While 3D bioprinting work has largely focused on improvements to the bioink itself, in recent years, a new class of 3D bioprinting materials has emerged that provides 'assistance' to the bioink. With help from assistive materials, bioinks which otherwise would be poorly suited for manufacturability may be 3D printed into larger and more complex shapes with high fidelity. Assistive materials in 3D bioprinting typically provide temporary aid to the bioink and then are removed from the printed structure. They can either serve as a medium into which the bioink is printed (support baths) or printed themselves (sacrificial inks).

Printing into a support bath, as opposed to onto a flat stage in air, keeps the printed bioink hydrated and suspended in place with lower interfacial tension. The support provided by the bath loosens the strict material requirements for bioink printability by preventing structural collapse and improving print fidelity [23]. An early example from 2006 of printing into support baths—also referred to as 'embedded printing'—was for cell spheroids deposited within a collagen hydrogel to maintain the spatial patterning of the spheroids until their fusion [25]. This fundamental concept was separately and simultaneously expanded upon to be suited for bioinks with a wide range of material properties by three different research groups led by Thomas Angelini, Jason Burdick, and Adam Feinberg. Their seminal papers on support baths were published in 2015 within months of each other [26–28]. In contrast to previous support baths, self-healing materials that mechanically recover after removal of an applied shear stress (e.g. movement of a nozzle) were developed to physically confine the bioink after extrusion. Thus, even weak materials with poor structural integrity could be printed as bioinks. Since these seminal works, the optimization of support baths to suit a variety of bioink materials has been of great interest to the bioprinting community [29, 30].

Sacrificial inks—also referred to as 'fugitive inks'—in 3D extrusion bioprinting have primarily been printed separately from the bioink to leave behind open void spaces once removed. Inspired by the use of materials in tissue engineering such as salt particles, beads, and sugars that create pores within biomaterial scaffolds [31], these sacrificial inks are commonly used to create hollow internal architectures within a print such as vasculature-like networks. Much of the pioneering work in 3D printed sacrificial inks for vascularized constructs was led by Jennifer Lewis. Building upon her work on using sacrificial inks to create microchannels within microfluidic devices [32], notable early demonstrations of sacrificial inks for 3D bioprinting were published in the early 2010s [33–35]. The hollow conduits formed by the sacrificial inks promote the transfer of oxygen and nutrients to cells, enabling the scale-up of prints with greater cell viability. Recently, a variation on this application of sacrificial inks has emerged, in which sacrificial inks are a component within bioinks. In this case, the sacrificial ink component temporarily changes the overall bioink material properties to increase printability, similar to additives (commonly viscosity modifiers) used in bioinks [36]. Unlike most viscosity modifiers historically used in bioprinting, however, these sacrificial ink components also have a removal mechanism to change the bioink properties to those desired after printing. More recently, they have also been used to tune the porosity of the print [37–39].

The use of assistive materials in 3D extrusion bioprinting indicates a paradigm shift in the field by dramatically expanding both the range of materials for bioprinting and the structural complexity of possible prints. Successful applications of assistive materials have already demonstrated an increase in both the achievable biological function and structural variety of printed constructs. Our review covers the primary

categories of assistive materials for 3D bioprinting: support baths and sacrificial inks. For each type of assistive material, we describe its advantages, material requirements, selected case-studies, and current challenges and opportunities. Finally, we conclude with a forward-looking perspective on the next generation of assistive materials in 3D extrusion bioprinting.

2. Support baths

The 3D bioprinting field has been limited by a lack of suitable materials for use as bioinks [5, 40, 41]. Since a bioink by definition contains a cellular component, printing variables (such as temperature, pressure, and pH) and bioink mechanical properties (such as stiffness and viscosity) must fit within a limited range suited for cell viability and function. In general, for soft tissue fabrication there exists a trade-off between printability and cell function, where stiffer, more viscous materials are able to retain their shape when printed, but softer, less viscous materials are more appropriate for promoting cell viability and processes such as migration, proliferation, and differentiation within a 3D matrix [42–46]. Therefore, there exists a 'biofabrication window' that represents a balance between printability and cell function, and it remains challenging to formulate bioinks that fit both these needs [22]. To widen the biofabrication window, there has been increased interest in printing bioinks into support baths rather than into air, as this improves print fidelity and loosens the strict material requirements needed to make inks printable. Using support baths enables the fabrication of more complex geometries that have the potential to better mimic *in vivo* architectures using materials that are optimized for cell culture rather than printability. Here, we outline the advantages of using support baths and the material properties that allow them to be used in this manner.

2.1. Advantages

Bioprinting into a gel-phase support bath offers several advantages over printing into air (figure 1). By physically confining the deposited ink and lowering the interfacial tension between the ink and the surrounding environment, the support bath can prevent structural collapse and enable printing of more complex features. This expands the number of possible structures that can be fabricated to include features such as windows and overhangs. These features can be readily constructed in a support bath because the medium provides both physical support during printing as well as a neutral buoyancy environment to prevent settling due to gravitational forces. Physical confinement of the ink has also been shown to increase print resolution and print fidelity, so the printed object more closely resembles the target computer-aided design (CAD) model [27, 28]. In addition, a support bath facilitates omnidirectional printing such that material deposition can occur in arbitrary directions and locations rather than in a layer-by-layer fashion [33]. This means that unconnected parts of the structure can be created independently and then joined afterwards, and that the printing needle can return to locations that it visited previously. Therefore, the variety of structures that can be fabricated is greatly increased in comparison to what is possible when printing into air [27].

Use of a support bath also expands the range of materials that can be made printable. By eliminating the requirement that the ink itself be self-supporting in air, a support bath enables printing of weaker, less viscous materials [47]. This can be useful to better match the ink material properties to those of the desired tissue type instead of needing to optimize the material properties to prevent instabilities and collapse after printing. However, if weaker inks are used, a crosslinking step—also known as 'curing'—typically needs to be employed *in situ* after extrusion so that the structure is stabilized in place and the bath can be removed. This crosslinking step will be dependent on the type of bioink used. For example, alginate inks can be crosslinked by divalent cations such as Ca^{2+}, collagen inks can be physically crosslinked through a neutralizing shift in pH, and methacrylated inks can be crosslinked through ultraviolet (UV) light exposure.

Therefore, two different crosslinking strategies can be employed: either the bath itself can include crosslinking molecules such as divalent cations, small-molecule diffusive crosslinkers, and catalysts, which can crosslink the ink as it is being printed, or the crosslinking step can be initiated after the entire structure has been printed, for example, by using UV light or thermal gelation [48–50]. In the case of crosslinking after the entire structure has been printed, use of a support bath offers another potential advantage. When printing in air in a layer-by-layer fashion, discontinuities often arise since the interface between sequentially deposited layers will not be seamless. In an aqueous support bath, a small amount of ink diffusion can occur prior to curing, allowing for individual filaments to more easily crosslink together into a cohesive structure. Finally, aqueous support baths keep the printed structure hydrated, preventing dehydration of the ink and improving cell viability. This becomes particularly important as the field strives toward creating full-size tissues and organs, as larger structures will require longer print times, which would leave more time for water loss if printing into air instead of an aqueous medium [35].

2.2. Material requirements

The material requirements for a support bath are twofold: first, the support bath should fluidize when the nozzle passes through it in order to leave a channel for ink deposition, and second, the material should recover and re-solidify after the nozzle is

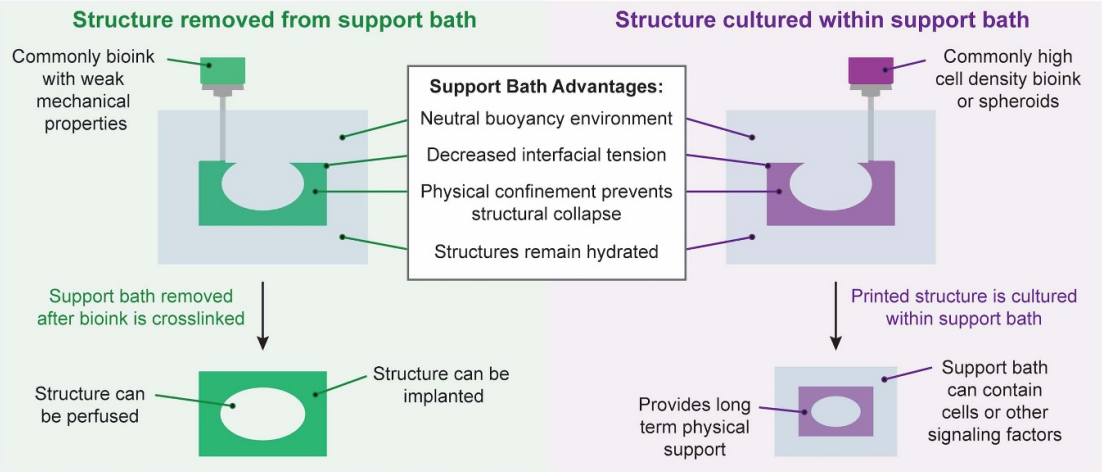

Figure 1. Schematic depicting the advantages of using a support bath for 3D bioprinting, where the printed structure is either removed from the support bath following printing or cultured within the support bath.

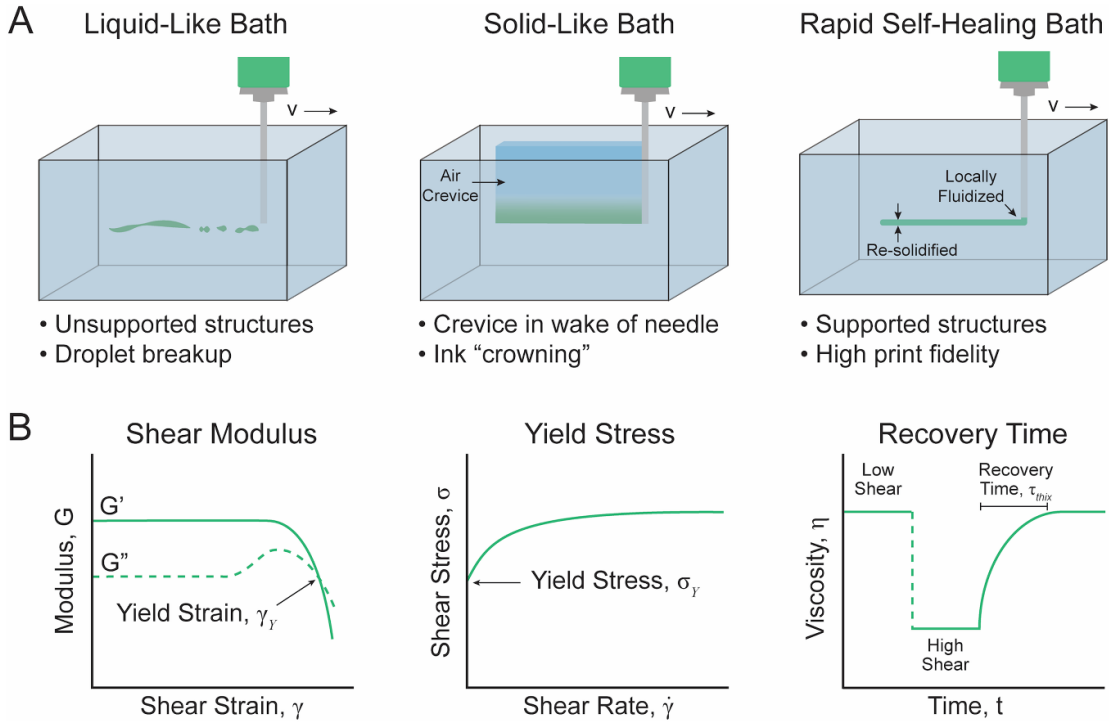

Figure 2. Material requirements for support baths. (A) The support bath material should ideally fluidize locally as the print nozzle passes through it, and then rapidly self-heal such that the bath re-solidifies after the nozzle is removed. If the bath is too liquid-like, the ink can undergo droplet breakup and printed structures can move due to buoyancy forces, resulting in unsupported structures. If the bath is too solid-like, the material may not recover quickly enough after the nozzle passes through, resulting in an air crevice in the wake of the needle into which deposited ink material can flow upwards in a process known as ink 'crowning'. (B) Common rheological measurements performed on support bath materials include determining shear modulus and/or yield strain from an oscillatory amplitude ramp experiment, the yield stress from a shear flow experiment, and recovery time from a step-down shear flow experiment.

removed, trapping the deposited material in place (figure 2). If the bath material exhibits more fluid-like properties, printed features can move due to buoyancy forces, and the ink can undergo droplet breakup [51]. Conversely, if the support bath material is dominated by solid-like properties, the bath may not re-fluidize after the nozzle passes through, creating a permanent crevice into which the ink material can flow upwards in a process known as 'crowning' [52]. Thus, there exists a set of material properties that strikes a balance between these two extremes, resulting in ideal ink deposition and confinement [53]. Here, we consider both the rheological properties and additional material characteristics that are critical for successful printing into support baths.

2.2.1. Rheological properties

2.2.1.1. Shear modulus

Support bath materials are typically viscoelastic and therefore exhibit both viscous and elastic behaviors in a time-dependent manner. The shear storage modulus, G', describes the elastic (solid-like) behavior of the material, and the shear loss modulus, G'', represents the viscous (fluid-like) behavior. The two components of the shear modulus are typically measured against time, frequency, or strain, and the value of the storage modulus is often reported for support bath materials (table 1). The storage modulus is commonly tuned by changing the concentration of the material, which can influence printed filament morphology. For example, in a Laponite (i.e. nanoclay) support bath, increasing the storage modulus led to improved print resolution and decreased the surface roughness of printed filaments [54]. A sufficiently high storage modulus (∼100 Pa) of the support bath has also been reported to aid in preventing structural collapse of the ink after printing [53]. Additionally, the relative magnitude of the storage modulus of the support bath (G_{bath}') in comparison to the modulus of the bioink (G_{ink}') can impact print quality [55]. If G_{ink}' is much greater than G_{bath}', then the nozzle may drag extruded material through the support bath, leading to poor print fidelity. However, if the support bath is too solid-like, and G_{bath}' is much greater than G_{ink}', then a crevice may form in the wake of the needle and the more liquid-like ink may flow upward. Finally, if the printed structure is cultured within the support bath, then the modulus of the support material should be tuned depending on the intended application. Most tissues in the body have stiffness values ranging from 0.1 to 100 kPa, so cells are typically cultured in similarly soft materials [56, 57]. Cells are also responsive to the mechanical properties of their surrounding matrix [58], and matrix stiffness has been shown to regulate cell spreading, migration, proliferation, gene expression, and differentiation [43–46]. Therefore, the modulus of the support bath can be optimized both to elicit the desired cell phenotype and to enable continued stability of the printed structure.

2.2.1.2. Yield stress

The support bath material should ideally behave as a yield stress fluid. The yield stress represents the stress required for flow initiation. This means that in the absence of an applied stress or at stresses below the yield stress, the material should exhibit solid-like properties. However, when a stress is applied above the yield stress, the medium should flow. In 3D bioprinting, this stress is applied by the tip of the printer nozzle. As the tip passes through the support bath, the material fluidizes locally and allows for controlled deposition of the ink. Then, the support bath material can re-solidify around the printed ink filament. Since no additional stress is applied following printing, the bath then behaves like a solid once more, holding the printed structure in place. Support bath yield stress behavior can typically be described by the Herschel-Bulkley model, which is a simple model to explain the behavior of non-Newtonian fluids where the shear stress (σ) is related to the yield stress (σ_0) and shear rate ($\dot{\gamma}$) through the fitted parameters k (consistency index) and n (flow index):

$$\sigma = \sigma_0 + k\dot{\gamma}^n.$$

The yield stress of a material can be found by fitting data from a shear flow experiment to the Herschel-Bulkley model. Reported values for support bath materials' yield stress vary greatly (table 1), but even if the yield stress is low, the presence of the yield stress itself is generally sufficient for expected support bath performance (i.e. local fluidization at the nozzle then a return to solid-like behavior to support the printed ink). Some research groups report the yield strain instead of the yield stress, so we present these values if the yield stress is not available (table 1). Yield strain can be determined from the crossover point of the storage and loss moduli (G'/G'') in a strain sweep experiment (figure 2(B)). However, it is difficult to compare yield strain values across studies, so reporting yield stress is preferred [59].

2.2.1.3. Recovery time

Once the printer's nozzle tip passes through the support bath material, the bath should ideally self-heal and re-solidify around the printed ink filament, holding it in place. The time it takes for the material to return to its initial state is referred to as the recovery time (or, alternatively, the self-healing time or thixotropic time). The recovery time can be determined by measuring either the viscosity or shear moduli in response to a step down in shear rate. The test begins at low shear, then a high shear rate is applied, and finally the shear rate is decreased to the original value. The time it takes for the viscosity or modulus to return to its original value is reported as the recovery time. The time scale of this re-solidification process should ideally be minimized; therefore, materials that display shorter recovery times have increasingly been chosen as support baths, since they can rapidly return to their initial solid-like state after abrupt changes in shear stress [60]. This ensures that the bioink material remains supported after printing.

2.2.2. Additional material considerations

2.2.2.1. Mechanism for removal

While the support bath is useful for fabrication, most applications require that the final printed structure be released from the support bath. Therefore, an additional constraint on the design of support bath materials is that they must have a mechanism for removal. Methods for support bath removal include changes in temperature to melt the support material, physical disruption by dilution and agitation, enzymatic

Table 1. Common materials used as support baths, their rheological properties, mechanisms for removal, and applications in 3D bioprinting.

Support bath material	Yield stress (Pa)	Yield strain (%)	Shear storage modulus (Pa)	Removal mechanism	Ink	Application	References
Acrylamide	0.1–10	—	1–55	Not removed	Collagen	Quantification of cell-generated forces in printed constructs	[63]
Alginate	—	∼25	∼200	Washing with water	Cell-only ink	Printing and differentiation of MSCs	[61]
Carbopol	9	—	64	Washing and agitation, multivalent cations	PDMS 184	Support bath material development	[64, 65]
Cell spheroids	10	—	∼200	Not removed	Gelatin	Perfusable patient-specific tissue	[66]
Gelatin	—	∼10	∼200–2000	Elevated temperatures (37 °C)	Alginate, collagen, fibrinogen, MeHA	Printing of at-scale human heart	[28, 62]
Gellan	1–2	—	∼100–400	Agitation in PBS	Alginate, gelatin, PEGDA	Support bath material development	[67]
HA-adamantane/HA-β-cyclodextrin	—	∼100	∼100–1000	Competitive binding of soluble β-cyclodextrin	HA-adamantane/HA-β-cyclodextrin	Support bath material development, perfusable microchannel networks	[26, 68]
Laponite	0.0015–16	—	∼1–1000	Washing with NaCl	Alginate/gelatin	Support bath material development	[54]
Pluronic	200	—	∼20 000	Lowered temperatures (4 °C)	Pluronic F-127	Perfusable microvascular networks	[33]

degradation, and disruption of crosslinks by ion chelation or a pH shift. Importantly, the removal mechanism should be as cell-friendly as possible so as to not damage the printed cells. Methods that induce large changes in pH, temperature, or ion concentration beyond that of physiological conditions may reduce cell viability and affect cell behavior. Alternatively, the bath itself may be incorporated into the final structure and can contain cells or other biological material. However, care should be taken to either include a perfusable network or limit the size of the bath, and thus the size of the structure, in order to meet the transport demands for cellular nutrition and oxygenation.

2.2.2.2. Granular gel support baths

Support baths composed of jammed microparticles have recently gained popularity, but additional material characteristics beyond the previously mentioned rheological properties must also be considered. In such systems, hydrogel microparticles are typically mixed with an aqueous, cell-compatible buffer and then centrifuged to compact the particles into a jammed state, often called a slurry. The packed particles can temporarily fluidize as the printer nozzle passes through, becoming unjammed, and can then return to a jammed state once the shear stress from the nozzle is removed. Therefore, these materials exhibit the requisite yield stress and self-healing behavior needed to effectively support printed structures. However, in addition to their bulk rheological behavior affecting print quality, factors such as particle size and shape can also influence print resolution and fidelity within microgel support baths [30, 61]. Larger particle sizes with greater polydispersity have been shown to lead to highly variable printed filament morphologies as the ink can flow into the interstitial space between adjacent support bath microparticles [62]. Decreasing the particle size and increasing their uniformity improved print resolution down to 20 μm and decreased the surface roughness of printed filaments, leading to printed structures that more closely resembled the intended CAD models.

2.3. Case studies

Here, we cover selected, illustrative examples of bioprinting into support baths, including cases both where the printed structure is removed from the bath and where the support bath serves as part of the final structure. For a more exhaustive list of published combinations of support bath and ink materials, we point the interested reader to another excellent recent review [23].

2.3.1. Support baths removed from final structure

Early demonstrations of printing into a support bath utilized single-phase yield stress fluids as the support medium. One of the first materials to be used was Pluronic F-127, a triblock copolymer that can undergo a temperature dependent phase transition from a physical hydrogel to a fluid at temperatures below 10 °C, enabling removal of the support material. Printing a Pluronic F-127 ink into a photocurable bath of Pluronic F-127 diacrylate facilitated the creation of interconnected, 3D microvascular networks [33]. However, since the gel-phase Pluronic F-127 is not self-healing, as the print nozzle passed through the bath, a void space the length of the nozzle was created. Therefore, a lower viscosity Pluronic F-127 fluid capping layer was added on top of the hydrogel reservoir so that the fluid could flow into the void. To avoid the need to use this additional fluid layer, materials that are both shear-thinning and self-healing have also been developed as support baths. For example, hyaluronic acid (HA) was modified with either adamantane (Ad) or beta-cyclodextrin (β-CD) so that when these two components were combined, they created a supramolecular, self-healing hydrogel support bath (figure 3(A)) [26]. A bioink was formed using the same guest–host hydrogels combined with cells, and the ink was printed directly into the support bath, enabling the fabrication of complex, multi-cellular structures. The support bath could be washed away by disrupting the guest–host bonds with the competitive binding of soluble β-CD [68]. Using such a support bath enabled printing of more complex hydrogel structures that contained internal void spaces and a higher degree of curvature than would be possible in air.

More recently, support baths consisting of jammed microparticles have gained popularity. An early demonstration of a jammed microparticle support bath used microgels consisting of a crosslinked polyacrylic acid copolymer, also known as Carbopol (figure 3(B)) [27]. After printing, the Carbopol support bath is removed by washing the printed structure in water with agitation. Any residual Carbopol can be further removed by the addition of multivalent cations, which react with the Carbopol microgels [69]. Another early example used jammed gelatin microparticles for freeform reversible embedding of suspended hydrogels (FRESH) printing [28]. Gelatin was chosen for its biocompatibility, thermoreversible properties, and low cost, and was shown to enable printing of weak biomaterials such as alginate, collagen, and fibrin into complex, anatomical structures. The gelatin particles are stable at room temperature, but can be melted at 37 °C, and therefore can be readily removed following printing. Follow-up work to reduce the dispersity and size of the gelatin microparticles improved printed filament resolution down to 20 μm and decreased the printed filament's surface roughness [62]. The improved rheological properties of these gelatin microparticles allowed for printing of several different ink materials and enabled successful printing of an at-scale, collagen-based human heart model (figure 3(C)). Recent work has expanded the range of support baths materials to include jammed

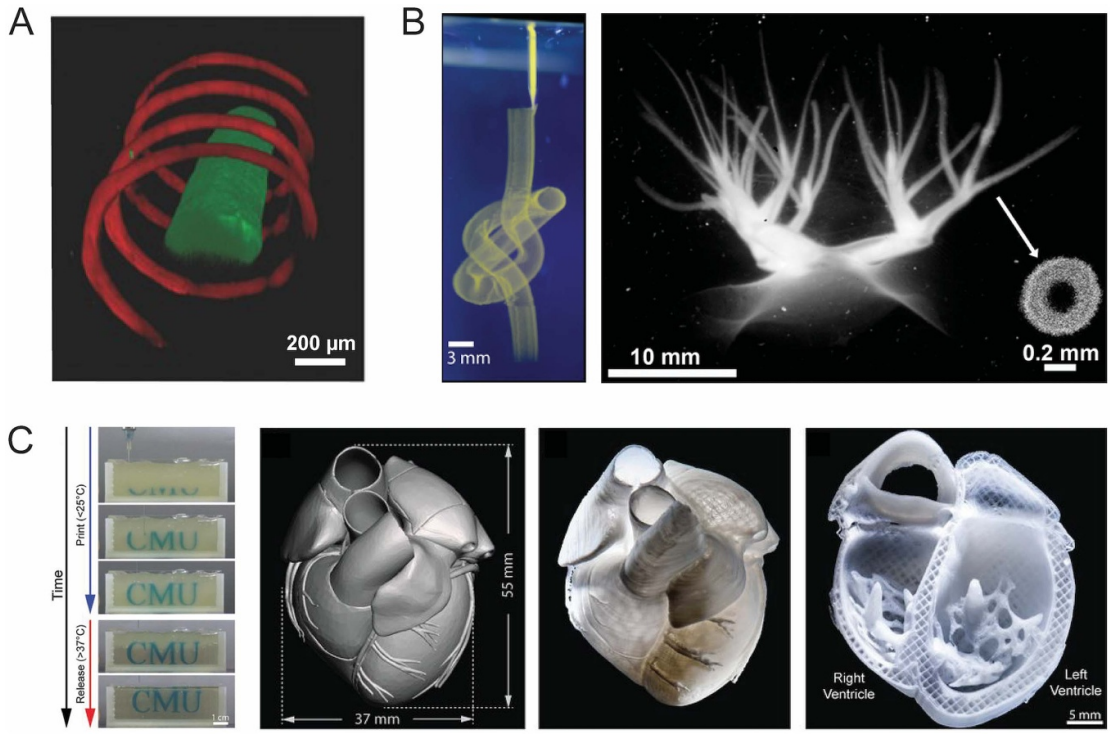

Figure 3. The use of a support bath allows for the creation of more complex bioprinted structures. (A) A shear-thinning and self-healing support bath based on supramolecular assembly through guest–host complexes allows for continuous printing in any direction of 3D space (green: filament of fluorescein-labeled ink, red: continuous spiral of a second, rhodamine-labeled ink). Reproduced with permission [26]. © 2015 WILEY-VCH Verlag GmbH & Co. KGaA, Weinheim. (B) A continuous knot and a highly branched network of hollow vessels are printed within a Carbopol granular gel support bath. Reproduced with permission [27]. Copyright 2015, AAAS. (C) A support bath composed of gelatin microparticles (FRESH 2.0) enables printing of an at-scale, collagen-based human heart. Reproduced with permission [62]. Copyright 2019, AAAS.

microparticles made from alginate [70], agarose [71], gellan [67], laponite nanoclay [54, 72], acrylamide [63], nanocellulose [73], and even slurries of cell spheroids [66].

2.3.2. Support baths as part of the final structure

While most bioprinting strategies call for removal of the printed structure from the support bath, some studies have incorporated the bath into the final fabricated construct. This alternative strategy can be used to pattern bioinks with higher cell densities and even cell-only inks, which might otherwise lack the appropriate mechanical properties to be self-supporting if the bath were removed [61, 74, 75]. The support bath continues to offer structural support throughout the culture period, and, as the 3D extracellular environment, can also provide biochemical and biophysical cues to the printed cells. In one example termed bioprinting-assisted tissue emergence (BATE), organoid-forming stem cells were printed into a viscous support bath of Matrigel and collagen (figure 4(A)). By patterning intestinal stem cells at a high cellular density, macro-scale, tissue-like constructs were made that self-organized into structures resembling lumens, crypts, and villi [74]. In another example, cell spheroids were spatially patterned by translating them through a shear-thinning hydrogel support bath made from HA-Ad and HA-β-CD (figure 4(B)). It should be noted that the spheroids were not extruded but were instead transferred using vacuum aspiration; however, the support bath material requirements remain similar to those for extrusion bioprinting, as the bath should still be shear-thinning and self-healing to allow for movement of the spheroid through the bath. This approach was used to spatially pattern cardiomyocytes and fibroblasts to create a printed microtissue model that recapitulated the functional behavior of scarred cardiac tissue [76].

Finally, the support bath itself can be composed of cells, as demonstrated by a technique termed sacrificial writing into functional tissue (SWIFT) [66]. This biomanufacturing method used organ building blocks (OBBs) made from patient-specific induced pluripotent stem cell (iPSC)-derived organoids and combined them with collagen and Matrigel to create an extracellular matrix/cell slurry with appropriate rheological behavior (i.e. stress-yielding and self-healing) to serve as a support bath. A sacrificial gelatin ink was then printed into the cell slurry, and, once removed, created a perfusable vascular network. Using iPSC-derived cardiac OBBs, a cardiac tissue model was created that fused and beat synchronously over the one-week culture time [66]. Altogether, these examples demonstrate how the support bath can be included in the final printed structure, can

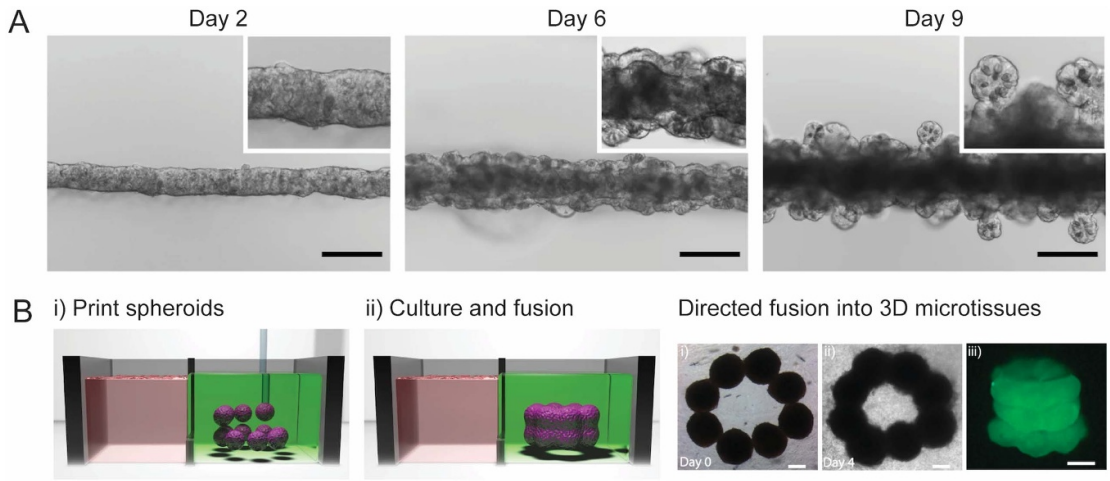

Figure 4. Culture within a support bath allows for printing of high cell density bioinks and spheroids. (A) In bioprinting-assisted tissue emergence (BATE), organoid-forming stem cells are printed at high cellular densities into a viscous support bath of Matrigel and collagen, which facilitates cellular self-organization into lumen and crypt-like structures. Scale bars, 200 μm. Reproduced with permission from Springer Nature [74], Copyright 2021. (B) 3D bioprinting of spheroids into rings within an HA support bath allows for spheroid fusion and microtissue formation over four days of culture within the support bath. Reproduced under the terms of the Creative Commons CC-BY License [76]. Published by Springer Nature.

help maintain structural support, and can provide an extracellular environment conducive to creating functional, tissue-like structures.

2.4. Remaining challenges and outlook

While printing into a support bath has become increasingly popular in academic laboratories and common support bath materials are now commercially available, there are still remaining challenges to using support baths, including (a) scaling up the size of printed structures, (b) visualizing printed structures, and (c) optimizing the support bath and bioink material properties in tandem.

Most prior demonstrations of printing into a support bath fabricated structures with relatively small sizes (i.e. mm to cm scale) [77], but creating large-scale, biologically relevant structures will be needed to make functional tissues and organs for transplantation. As the size of the desired structure becomes larger, the volumes of the support bath, bioink, and print container also increase. Printing into larger support bath containers will require the use of longer needles. Since print resolution is correlated with needle diameter, needles with relatively small internal diameters (i.e. 80–150 μm) are commonly used to fabricate more intricate structural features [62, 78, 79]. The combination of longer needles and smaller internal diameters presents a problem, as the needle can be more easily deflected at the bottom of the support bath, especially if the bath exhibits a higher yield stress and more resistance to flow. One possible solution is to use reinforced needles, but careful tuning of the support bath material properties will most likely also be needed as print size increases [23]. In addition to the increased support bath volume, larger structures will also require longer print times. Therefore, cells will spend more time within the bioink or within the support bath itself and out of their ideal culture environment, which could lead to increased cell death. This could be mitigated by decreasing the temperature of the bioink and/or support bath to slow cell metabolism, although this necessitates that the support bath maintains the appropriate rheological properties at these reduced temperatures. Thus, further optimization of currently available support bath materials may be needed when printing at-scale tissues and organs.

Another challenge when printing into a support bath rather than in air is the relative difficulty of visualizing the bioink as it is being extruded. If the support bath is not optically clear, it can be hard to identify issues such as clogged needles, bubbles, or defects during the printing process. In addition, as the complexity of the print increases to better mimic *in vivo* structures, more internal features will likely be present which cannot be seen through visual inspection of the outside of the print. New approaches to imaging printed structures both during and after the printing process to verify print fidelity will be needed for such structures. Some methods already in development include volumetric imaging modalities such as optical coherence tomography and *in situ* confocal microscopy [80].

Finally, while the availability and choice of gel-phase support bath materials has grown rapidly in the past few years, there is no universal support bath material that will work for every bioink formulation. Instead, the support bath material properties often need to be optimized for each particular application [81]. Further standardization of reported rheological properties and print quality metrics will be useful in determining the interplay between the mechanical

properties of the bioink and support bath and how these affect the final print fidelity and resolution. In addition, while the printed structure may match the intended CAD structure while in the support bath, changes may occur during the removal process or over time in culture due to swelling, erosion, or cell-generated forces acting on the printed material. For example, bioinks formulated using alginate may have good print fidelity while in a support bath containing Ca^{2+} ions which crosslink the ink, but could erode over time once the structure is removed from the support bath and cultured in a low calcium environment [82]. Even when the support bath is not removed, bioprinted microbeams were observed to evolve over time due to cell-generated forces, and the type of change that occurred was dependent on the construct size, cell density, polymer content of the bioink, and material properties of the support bath [63]. Therefore, further opportunities exist to tune the support bath properties to ensure that the printed construct evolves over time to suit the intended biological application.

3. Sacrificial inks

Sacrificial inks are another type of assistive material for 3D bioprinting that have been used separately or in conjunction with support baths to aid in the creation of complex patterns and open void spaces in the internal architecture of the print. Like the majority of support baths, sacrificial inks are by definition not a component of the final bioprinted construct. Sacrificial inks are either (a) printed separately from a bioink or (b) incorporated within the bioink. After solidification of the surrounding non-sacrificial material into its intended geometry, sacrificial inks undergo a removal mechanism to be cleared away from the construct.

3.1. Sacrificial inks printed separately from the bioink

3.1.1. Advantages

Sacrificial inks provide temporary support for the surrounding bioink material during the 3D bioprinting process as well as introduce patterns of removable material from the bulk structure (figure 5). When bioinks are printed in air rather than a support bath, sacrificial inks serve as physical support for overhangs and hollow structures until the bioink is crosslinked to be self-supporting [37]. This function is similar to support baths, which prevent the collapse of a printed bioink geometry. On the other hand, when sacrificial inks are printed into a support bath, the bath commonly becomes a component of the final print, with channels left in the place of the sacrificial ink [83]. In this case, a printed bioink is not necessarily used in conjunction with the support bath and sacrificial bioink, especially if cells are encapsulated within the support bath and/or are later perfused through the structure to line the inner channels left by the sacrificial ink [34, 66].

The primary application of sacrificial inks in bioprinting thus far has been to create perfusable networks, often mimicking vasculature. The formation of vasculature within 3D tissue models is highly desired, especially for large-scale constructs, because the majority of cells in the human body are less than 200 μm from a supply of blood [24]. Therefore, the presence of perfusable networks mimicking vasculature will be especially essential for bioprinting full-scale organs [84, 85]. Since cell survival is contingent on access to oxygen and nutrients, the hydrogel size and shape is restricted in part by the distance of cells from a free hydrogel surface. Sacrificial inks have been leveraged to create perfusable channels that allow for fresh medium to be pumped through the print, increasing oxygen and nutrient transfer to cells. With this approach, the overall size of the cell-laden hydrogel is less limited by diffusion from outer surfaces of the bulk hydrogel, allowing for bioprinting of thick, vascularized, tissue-like constructs that do not suffer from necrotic cores [86].

3.1.2. Material requirements

Unlike support baths, sacrificial inks are extruded during the printing process and therefore are subject to similar rheological design requirements as bioink materials, which have been detailed in recent review papers [5, 29, 36]. The rheological properties of a material affect its printability, defined here as its ability to be extruded into continuous filaments that maintain their shape fidelity [21]. For example, hydrogel inks for 3D extrusion printing should have (a) a high enough viscosity to prevent droplet formation, (b) a yield stress to remain solid-like prior to printing but then flow during extrusion, and (c) shear-thinning and self-healing behavior such that the viscosity decreases during extrusion through the needle and recovers after the strain is reduced [5]. Sacrificial inks, however, additionally demand a removal mechanism that allows the sacrificial material to easily disassociate from the bioprinted construct. Removal mechanisms include dissolution in aqueous media [34, 87], physical extraction [88–90], sol-gel transitions through temperature change [35, 66, 86], and dissolution with chelators [91, 92] or small molecule competitors [68].

Since bioprinted constructs contain cells, the sacrificial ink material and the method of its printing and removal should not be cytotoxic. For example, molten sacrificial inks that require printing at very high temperatures cannot be printed in contact with a cell-laden bioink until after cooling, due to cell death at super-physiological temperatures. Similarly, melting sacrificial materials post-printing at very high temperatures for removal from the construct would induce cell death [93]. Methods to remove sacrificial inks from prints with greater cell compatibility are

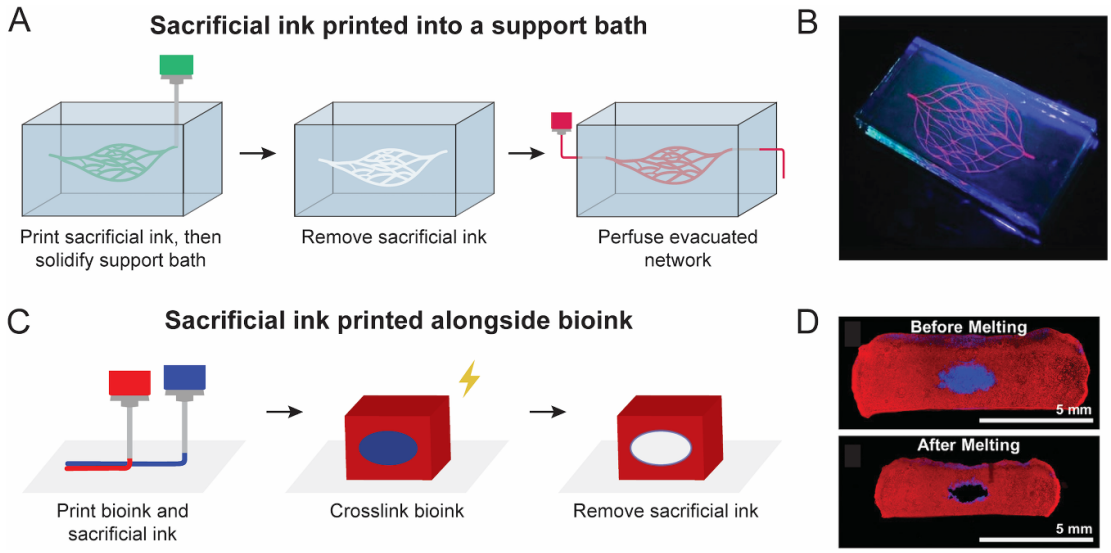

Figure 5. Sacrificial inks may be printed into a support bath and/or alongside a bioink to allow for the formation of internal void structures. (A) To create a perfusable network within a support bath, sacrificial inks are extruded into a specified geometry and then evacuated from the surrounding material after its solidification, leaving behind open channels. (B) A Pluronic sacrificial ink (dyed red) is used for omnidirectional printing of a microvascular-like pattern into a gel-based support bath. Reproduced with permission [33]. © 2011 WILEY-VCH Verlag GmbH & Co. KGaA, Weinheim. (C) Sacrificial inks printed alongside bioinks offer structural support during printing for overhangs or hollow internal features. Once the bioink is crosslinked into its final geometry, the sacrificial ink is removed, leaving hollow voids in its place. (D) A sacrificial ink of gelatin microgels (dyed blue) is printed alongside a gelatin methacryloyl (GelMA) microgel bioink material (dyed red). After photocrosslinking of the GelMA, the sacrificial gelatin microgels patterned internally are melted away at 37 °C. Reproduced with permission [37]. © 2021 WILEY-VCH Verlag GmbH & Co. KGaA, Weinheim.

Table 2. Common materials for sacrificial inks and their mechanisms for removal. By definition, sacrificial inks are eliminated from the print.

Sacrificial ink material	Removal mechanism	References
Agarose	Physical extraction	[88–90]
Alginate	Chelating agent	[91, 92]
Carbohydrate glass	Dissolution in aqueous solution	[34]
Carbopol	Washing with water	[95]
Gelatin	Elevated temperatures (37 °C)	[66, 96–98]
Pluronic	Lowered temperatures (4 °C)	[35, 86]
Poly(vinyl alcohol)	Dissolution in aqueous solution	[87, 99]

included in table 2. The biochemical properties of the sacrificial ink, however, are not as crucial as for the bioink, since the sacrificial material is removed from the print and typically does not include encapsulated cells. On the contrary, it may be beneficial for cells within the bioink to not adhere to the sacrificial ink that will be removed, so that the cell content and printed shape of the construct are preserved [94]. Therefore, sacrificial inks are often made from more biologically inert materials than bioinks (table 2).

3.1.3. Case studies

While the majority of bioinks are crosslinked into hydrogels, which simulate the 3D extracellular matrix for encapsulated cells, sacrificial inks rarely contain cells. Therefore, some non-hydrogel materials with harsher manufacturing conditions have also been leveraged as sacrificial inks, especially to create sacrificial molds. In one instance, a formulation of molten carbohydrates (>100 °C) was printed with thermal extrusion printing—also known as 'fusion deposition modeling'—and solidified at room temperature into carbohydrate (sugar) glass. Though more commonly used as a sacrificial material for 3D printing with non-biological materials [100], carbohydrate glass filaments were printed into a self-supporting lattice which was subsequently encased by a cell-laden hydrogel (figure 6(A)) [34]. The high water content in the hydrogel induced the dissolution of the embedded carbohydrate glass to create a lattice of perfusable, hollow channels. Compared to cells within a control hydrogel slab, cells within the hydrogel with channels suffered less from the formation of necrotic cores and better sustained their metabolic activity; this improvement became more pronounced with increasing cell density. While notable, this demonstration of carbohydrate glass as a sacrificial ink material for 3D bioprinting was limited

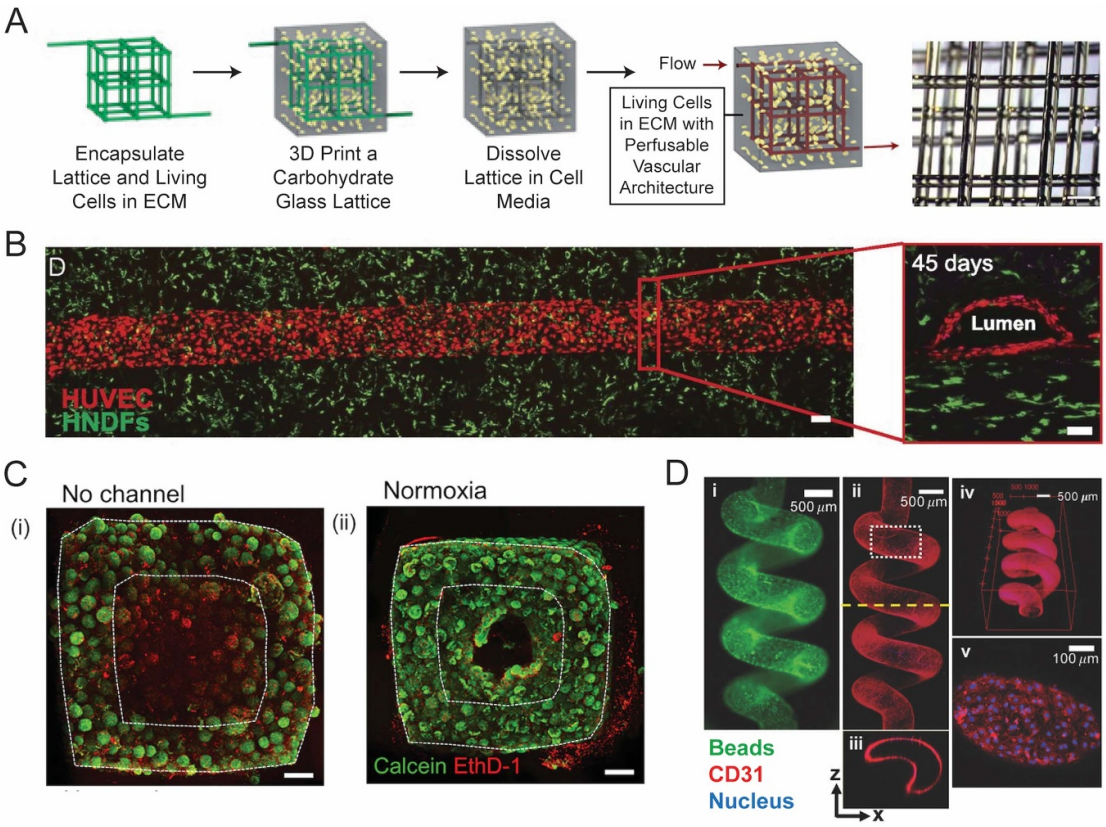

Figure 6. Sacrificial ink materials enable 3D bioprinting of voids and channels. (A) A water-soluble carbohydrate glass is printed into a lattice and encased within a cell-laden hydrogel. Contact with aqueous media causes the carbohydrate glass filaments to dissolve, leaving behind open channels that are then perfused with cell culture media and endothelial cells. Adapted and reproduced with permission [101]. Copyright 2012, Springer Nature. (B) An endothelialized, perfused channel after removal of a Pluronic sacrificial ink supports the surrounding fibroblasts within a thick tissue-like construct over 45 days. Scale bars, 100 μm. Reproduced with permission [86]. Copyright 2016, National Academy of Sciences. (C) Without a channel allowing for perfusion through an embryoid body tissue, a necrotic core is formed within 12 h. Bulk cell survival through the tissue-like construct is significantly improved when channels are introduced via a gelatin sacrificial ink for perfusion of normoxic media. Scale bars, 500 μm. Reproduced with permission [66]. Copyright 2019, AAAS. (D) A spiral microchannel printed from a guest–host sacrificial ink allows for perfusion with fluorescent beads and seeding with endothelial cells. Reproduced with permission [68]. © 2018 WILEY-VCH Verlag GmbH & Co. KGaA, Weinheim.

in the achievable geometric complexity of the filaments. Since the filaments were printed into air without other support structures, the channel pattern formed was a simple rectangular lattice. To achieve more complex channel shapes, in another example of thermal extrusion bioprinting, a 3D branched sacrificial structure was printed into air from poly(vinyl alcohol) (PVA) using poly(lactic acid) (PLA) as a support material to prevent collapse during printing [99]. After printing, the PLA support was removed with chloroform washes, leaving behind a water-soluble PVA sacrificial mold. Similar to the carbohydrate glass lattice [34], the PVA sacrificial mold was then encased within a cell-laden hydrogel, dissolved in the aqueous medium to leave behind channels, and perfused with endothelial cells. In addition to uses for vascularization, similar synthetic polymers have been used to provide structural support to bioinks for anatomically shaped tissue constructs with overhang geometries, including an ear and distal femur [87].

For gel-based sacrificial inks, one of the early examples was agarose, a naturally derived polysaccharide. In one instance, printed agarose rods served as a temporary support to hold the shape of multicellular spheroids or cylinders while the cells fused into tubular structures over the course of five to seven days [88]. After cell fusion, the sacrificial agarose rods were manually pulled out from within the tubes. In other examples, heated agarose was extruded at room temperature to form hydrogel microfibers in a pre-specified branched pattern [89, 90]. A cell-laden photopolymerizable hydrogel precursor was then cast around the sacrificial ink network and exposed to UV light. Since the agarose microfibers did not adhere to the neighboring photocrosslinked material, the agarose could be extracted either via aspiration with a mild vacuum or manual pulling, leaving behind interconnected, hollow channels. To more closely mimic vasculature, the conduits were infused with endothelial cells that formed monolayers along the inner surface of the hollow network. However, the structure of the vascular networks made using agarose sacrificial inks is limited by the physical extraction removal mechanism, since

branches must be open-ended and mechanical forces may be exerted on the adjacent bioink during extraction, causing disruption to the material structure [88, 90]. Therefore, the use of sacrificial materials that disintegrate with temperature changes or the addition of small molecules have been attractive for enabling more complex void geometries and convenient, mild extraction conditions.

Pluronic and gelatin are two of the most commonly used and successful thermoreversible polymers for sacrificial inks in bioprinting. Due to its shear-thinning nature and high viscosity, Pluronic has good printability and shape fidelity, thus being well-suited for an extrudable sacrificial ink. In one example, Pluronic was co-patterned along with two gelatin methacryloyl (GelMA)-based, fibroblast-laden bioinks [35]. After printing, the Pluronic sacrificial ink was liquified by lowering the temperature to 4 °C and evacuated from the print, leaving behind open, embedded microchannels that were subsequently endothelialized to line the lumen. In a follow-up study, a construct of bioengineered bone greater than 1 cm in thickness was fabricated by printing a mesenchymal stromal cell (MSC)-laden bioink of gelatin/fibrinogen and casting fibroblasts in the interstitial space (figure 6(B)) [86]. The construct was vascularized using a Pluronic-based sacrificial ink to create directly perfusable channels, which were again endothelialized. This thick and vascularized tissue-like construct was viable for more than six weeks, and the ability to perfuse growth factors through the channels in the construct promoted the differentiation of MSCs toward an osteogenic lineage. An alternative thermoreversible sacrificial ink is gelatin. Rather than liquification by cooling as with Pluronic, gelatin melts at elevated temperatures. Examples of gelatin used as a sacrificial ink include gelatin printed between layers of collagen to create fluidic channels [97, 98] and the SWIFT technique of printing a gelatin network embedded within a slurry of cell spheroids (described in section 2.3.2 above) (figure 6(C)) [66]. Upon raising the temperature to 37 °C, the gelatin was easily liquified and drained from the construct to create a perfusable internal architecture through which oxygenated media was pumped.

A final class of materials used as sacrificial inks are those with reversible or dynamic crosslinking mechanisms. Alginate rapidly crosslinks in the presence of divalent cations, commonly calcium. For use as a sacrificial ink, alginate may be uncrosslinked for easy removal with the introduction of a calcium chelating agent [91, 92]. In another approach that includes a dynamic crosslinking mechanism, HA was functionalized with guest–host pairs of Ad and β-CD (figure 6(D)) [68]. After printing the modified HA into a photocrosslinked hydrogel-based support bath, the guest–host bonds stabilizing the sacrificial ink were disrupted by the addition of excess β-CD in solution, which competed for the binding crosslinking sites on Ad-HA. The sacrificial ink could then be washed away, leaving behind well-defined channels within the support hydrogel.

3.1.4. Remaining challenges and outlook

While notable examples of 3D bioprints leveraging sacrificial inks to create voids and channels have been demonstrated, a few key challenges still remain in the development and use of sacrificial inks. These include printing considerations, achievable resolution, and removal of the sacrificial ink for perfusable channels.

For sacrificial inks used as support for overhangs or channels for bioinks printed into air, the material must be optimized for printability and structural stability. When sacrificial inks are printed alongside a bioink and incorporated within the structure of the print, a separate nozzle for the sacrificial ink is required. The need for multiple printing nozzles demands more specialized hardware and software than simple single-nozzle 3D bioprinters, even to make a print from a single bioink. Thus, if the sacrificial ink's primary role is to provide support for large features of the geometry, printing the bioink into a support bath rather than using a sacrificial ink may be a more efficient and effective method for supporting complex geometries until the bioink is solidified.

The smallest feature size achievable for printed inks is determined in part by the size of the needle through which the ink is extruded, limiting the possible resolution. In the case of vasculature formed by printing sacrificial inks, the needle size will affect the diameter of the channels. The diameters of blood vessels in the human body range from large arteries (~25 mm for the aorta) down to tiny capillaries (5–10 μm) [102]. Therefore, while 3D extrusion bioprinting with sacrificial inks can create vascular-like networks traversing thick constructs, hierarchical sized channels that closely mimic those in the human body have yet to be demonstrated. In particular, current methods of 3D extrusion printing with sacrificial inks are not yet well-suited for directly creating microvasculature due to the resolution limitations of printing. However, improvements to support baths have increased resolution of printed bioinks, achieving filaments with a consistent diameter down to ~20 μm [62]. Future work in the field to improve vascularization of prints may involve optimization of the material surrounding the sacrificial ink (either the bioink or support bath) or inclusion of growth factors or small molecules to promote formation of microvasculature from endothelial cells during post-printing culture and maturation of the construct.

Finally, removal of the sacrificial ink and perfusion of channels with cells becomes more challenging as the channel diameter decreases and the complexity (e.g. amount of branching and curves) of the printed network increases. The removal method for the sacrificial ink must be selected such that it is reliably

eliminated from the print while simultaneously not disrupting the surrounding cells and material in the print. Additionally, when cells are perfused through the network, they must remain viable and evenly distributed [35]. Inclusion of cells within the printed sacrificial ink may improve the evenness of cell distribution within channels, especially for small channels far from the inlets which may be poorly perfused. In this case, however, care must be taken to ensure the cells adhere to the print material rather than to the sacrificial ink. Otherwise, there is a risk that the cells will be eliminated from the print along with the sacrificial ink rather than line the inner walls of the channel as desired.

3.2. Sacrificial inks as a bioink component

3.2.1. Advantages

In a different application of sacrificial inks as assistive materials, sacrificial components have been blended directly into the bioink to (a) temporarily increase the viscosity to slow cell sedimentation and improve printability and/or (b) introduce porosity to the printed bioink to improve spreading, migration, and proliferation of encapsulated cells. In all cases, once the primary bioink material is crosslinked into place after printing, the sacrificial ink component is eliminated (figure 7).

Increasing the viscosity of the bioink prior to and during printing has a couple of key advantages. Bioinks with higher viscosity have greater resistance against gravity pulling cells toward the bottom of the syringe prior to printing [103, 104]. Avoiding cell sedimentation allows for a more even distribution of cells within the print, especially for large constructs with long print times [105]. The viscosity of the bioink also affects its ability to be extruded as a continuous filament. For bioinks printed layer-by-layer into air, higher viscosities improve print resolution and the ability of the printed filaments to be self-supporting [106]. Historically, to increase the viscosity of a bioink, high-density polymer networks or viscosity modifiers such as cellulose nanofibers and silk fibroin have been used [103, 107]. However, materials with high viscosities may hinder the essential activities of encapsulated cells by affecting nutrient diffusion and cell-matrix interactions [108–110]. Therefore, a reversible viscosity change of the bioink is often desired to reduce the need to compromise between printability and biocompatibility, especially for mimicking soft tissues. Thus, sacrificial inks can serve as secondary networks within the bioink to increase viscosity during printing but then be removed afterward to revert the bioink to the material properties optimized for cell culture. With this strategy, the biofabrication window of materials that can be used as the bioprint scaffold material is expanded to include materials with high biomimicry and otherwise poor extrudability or structural stability [96, 111].

In addition, porosity is an important matrix property that affects many aspects of cell behavior and can be tuned by including a sacrificial ink component. Micro- and macroporous hydrogels with interconnected voids have several advantages over nanoporous hydrogels for 3D cell culture, including improved exchange of nutrients and increased amounts of cell growth, spreading, and migration [31]. In the field of tissue engineering, porogens—often leachable solid particles—have historically been used to create pores within molded constructs [112, 113]. However, solid particles with large sizes are not well-suited for 3D bioprinting due to their tendency to clog nozzles during extrusion. Therefore, there has been growing interest in extrudable sacrificial ink components incorporated into the bioink that both maintain printability and create pores after removal. Notably, sacrificial microgels [37] or a removable, immiscible aqueous phase [38, 39] within the bioink have enabled printing constructs with interconnected pores.

3.2.2. Material requirements

The addition of sacrificial ink components to bioinks must change the properties of the overall bioink to be suitable for extrusion. A number of rheological properties are especially of interest to allow for extrudability of bioinks, which are commonly hydrogels [5, 29, 36]. These rheological properties are similar to those summarized in section 3.1.2: Material requirements for sacrificial inks printed separately from bioinks. However, since sacrificial materials contained within a bioink include encapsulated cells as an intrinsic component, cell compatibility considerations are also important to maintain high cell viability during printing.

To be printed into air, hydrogel bioinks should have a yield stress to not flow in the syringe until pressure is applied and a sufficiently high viscosity to be extruded in continuous filaments [114, 115]. Cell sedimentation in the syringe prior to printing decreases for bioinks with higher yield stress and viscosity [104]. However, materials with higher yield stress require larger pressures to extrude, and materials with higher viscosity increase shear stress during extrusion. Since both of these factors can negatively impact cell viability [59, 116], care must be taken to strike a balance between sufficient printability and cell viability. Finally, the bioink should be shear-thinning and self-healing. Many shear-thinning bioinks will shear at the wall of the nozzle during printing, allowing the material to pass through the nozzle as a relatively undeformed plug. Thus, encapsulated cells are protected from mechanical forces that may cause cell death [117, 118]. The recovery of the viscosity of the bioink after printing improves print fidelity and shape retention until the final crosslinking steps are completed [119].

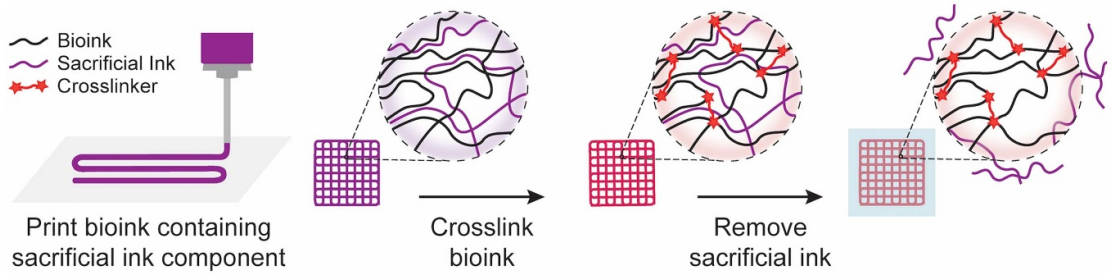

Figure 7. Sacrificial ink components within the bioink increase its viscosity to assist in filament extrusion and improve the structural stability of the sequentially printed layers. Once the bioink has been printed and crosslinked, the sacrificial component is removed from the construct, leaving behind the desired bioink material.

Since the sacrificial ink component of the bioink is intended to be removed from the final print, the sacrificial material must have a removal mechanism, similar to sacrificial inks printed separately from the bioink. The removal mechanism should be as gentle as possible to not disrupt the surrounding bioink material and cells. Furthermore, the removal method should ideally be effective enough that little residue of the sacrificial component is left behind in the matrix, if the primary non-sacrificial bioink component on its own or with a certain porosity was the material optimized for cell culture.

3.2.3. Case studies

A range of sacrificial ink materials have been used to make other materials printable, including the addition of alginate, agarose, and gelatin to bioink formulations [69, 94, 96, 111]. A couple of notable recent examples have attempted to design 'universal' sacrificial bioink components to improve the printability of bioinks for better shape fidelity. In one case, a sacrificial bioink component was produced from a mixture of alginate and agarose and added to a cell-laden GelMA bioink [94]. Umbilical cord vein-derived smooth muscle cells within the GelMA-based bioink were 3D bioprinted into tubular models, which were tested for cell viability and shape fidelity. The polysaccharide sacrificial components, which were not crosslinked, spontaneously eroded away from the print over the course of a couple days in cell culture medium at 37 °C. In another example, the thermal-reversible gelation of gelatin was exploited to print a range of biomaterials at polymer concentrations that typically would not otherwise be printable (figure 8(A)) [96]. To do so, a polymer functionalized with a photocrosslinkable moiety was mixed with gelatin, forming a polymer network with two different gelation mechanisms. The gelatin network allowed for the ink to become extrudable and stable at low temperature. Following photocrosslinking of the printed structure, the gelatin could be removed by heating without affecting the photocrosslinked network. This strategy allowed for the consistent printability of 12 different polymers (photocrosslinkable forms of gelatin, HA, chondroitin sulfate, dextran, alginate, chitosan, heparin, and polyethylene glycol) that were not otherwise extrudable at their desired concentrations. A range of 3D structures were printed, including a pyramid and trifurcated tubular construct, and the printed hydrogels supported a culture of astrocytes. With this approach of using sacrificial inks within bioinks during printing, the biofabrication window is broadened to include a greater range of bioink materials.

Furthermore, sacrificial components within bioinks may be used to control the microstructure of the print, including porosity. One recent demonstration decoupled the printability and the void fraction of the printed scaffold using a bioink material made from blends of photocrosslinkable GelMA microgels with sacrificial gelatin microgels (figure 8(B)) [37]. The concentration of the slurry of jammed microparticles was optimized for printability and held constant, while the ratio between the sacrificial and non-sacrificial components was modulated. Once the bioink material was printed into a self-supporting structure into air and exposed to UV light to crosslink the GelMA microgels, the sacrificial gelatin microgels were melted away at 37 °C, leaving behind interconnected void spaces within the printed bioink material. By using multiple inks with different amounts of sacrificial microgels within a single construct, heterogeneous patterns were achieved with different amounts of gel porosity. Endothelial cells were seeded on top of the prints and migrated farther into printed scaffolds with increased void space. Another notable example of using a sacrificial ink component to create interconnected pores within a bioprint involved an aqueous two-phase emulsion bioink comprised of photocrosslinkable GelMA and a sacrificial polyethylene oxide (PEO) phase [38, 39]. After exposure to UV light to crosslink the GelMA, the PEO was removed by immersing the construct in PBS for 24 h. Hepatocellular carcinoma cells, endothelial cells, and embryonic fibroblasts encapsulated within the porous constructs exhibited enhanced cell viability, spreading, and proliferation compared to the 'nonporous' control hydrogel [38]. Thus, sacrificial

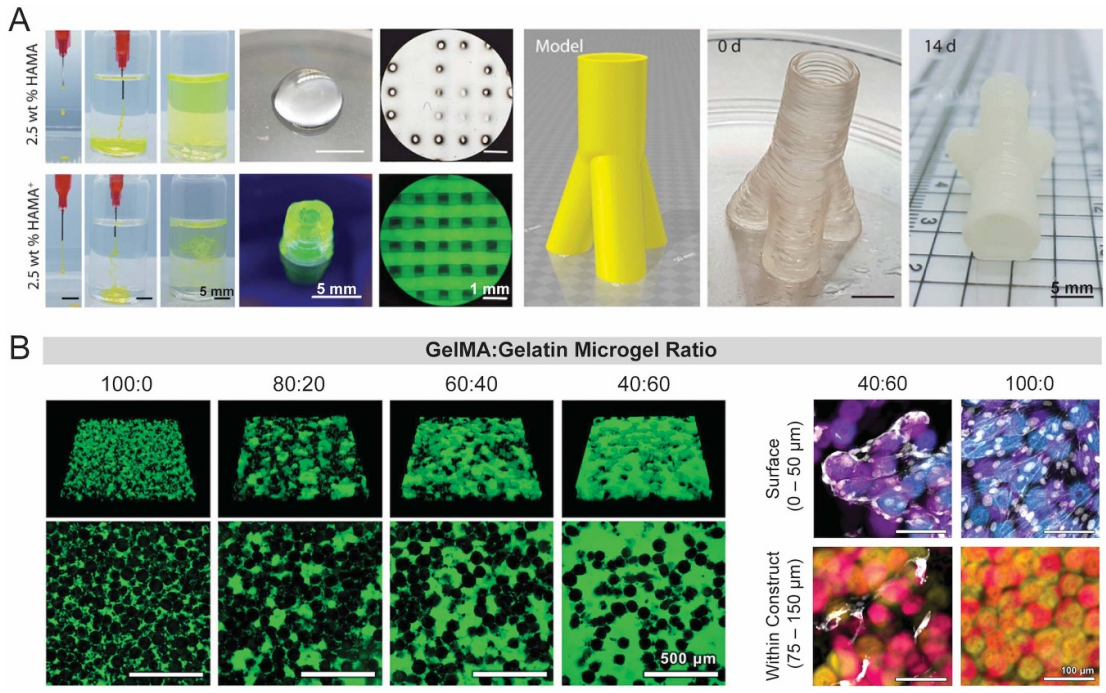

Figure 8. Sacrificial ink components within the bioink expand the range of printable materials and allow for tuning of the porosity of the final construct. (A) The addition of a gelatin sacrificial ink component to methacrylated hyaluronic acid ($HAMA^+$) improved the stability of extruded filaments and the printability of tubular and lattice constructs, compared to HAMA without the sacrificial ink component ($HAMA^-$). A bioink of $GelMA^+$ and osteogenic sarcoma cells was printed into a hollow trifurcated tube shape with overhanging walls that maintained its printed geometry over 14 days of cell culture. Reproduced with permission [96]. Copyright 2020, AAAS. (B) With increasing amounts of sacrificial gelatin microgels within a GelMA microgel bioink material, the void space (green) increased. Endothelial cells seeded on top of the hydrogels spread along the interconnected voids created by the sacrificial gelatin microgels and migrated farther into the construct than a print of only GelMA microgels. Reproduced with permission [37]. © 2021 WILEY-VCH Verlag GmbH & Co. KGaA, Weinheim.

materials may be leveraged to not only increase printability of materials but also to control microscale features within the print to affect cell behavior.

3.2.4. Remaining challenges and outlook

Since a key advantage in the concept of using sacrificial inks within bioinks is that the sacrificial component is eliminated after printing and crosslinking of the bioink, an important challenge is ensuring a controllable removal of the sacrificial material. Thus far, it has commonly been desired that the removal of sacrificial material be fully completed to restore the bioink properties to those optimized for cell culture. The residual amount of sacrificial material in the bioink after its removal mechanism is triggered should be monitored over time due to possible effects on the end application of the bioprint. For example, the amount of sacrificial gelatin released from bioinks depended on the primary bioink material type, polymer concentration, and crosslinking density, and the amount of sacrificial gelatin released increased from day 1 to day 15 of culture [96]. Remaining sacrificial material may influence cells in ways that differ from those of the pure, intended bioink material and thus should be considered as part of the matrix when drawing conclusions about the effects of matrix properties on encapsulated cells. On the other hand, future opportunities may exist using sacrificial inks with a purposefully delayed or prolonged removal mechanism. As was demonstrated with sacrificial gelatin microgels within the bioink material that left behind void spaces, sacrificial ink components may change the microstructure of the print [37]. Thus, exciting future opportunities leveraging sacrificial inks within bioinks may include temporal studies in which a change in the overall bioink material properties is induced at a specified timepoint or occurs gradually, depending on the timing and rate of the sacrificial ink removal mechanism. Additional perspective on the selection of 'bio-inert' versus 'biofunctional' sacrificial materials and their removal mechanisms—which also apply to the design of other assistive materials in 3D extrusion bioprinting—will be provided in section 4 below.

4. Future perspective and conclusion

Engineered assistive materials (i.e. support baths and sacrificial inks) for 3D extrusion bioprinting have elevated the achievable geometric complexity and biomimicry of printed constructs in recent years. Future improvements in the field of 3D bioprinting will likely rely on the improved design and use of these assistive materials. In particular, opportunities lie in tuning the biofunctionality of assistive materials and their removal mechanisms.

Thus far, the selection of materials for support baths or sacrificial inks has been largely guided by the physical properties of the material, such as its rheological properties and facile removal. As the field of 3D bioprinting matures, greater consideration should be given to the biofunctionality of the assistive material to control its interactions with cells. For acellular assistive materials adjacent to or within a bioink containing cells, materials that lack cell-adhesive ligands may be preferred to prevent the adherence of cells to the assistive material. This avoids the subsequent removal of cells from the constructs along with the eliminated assistive material, such that the cell density within the construct is not affected. For other applications, designing the assistive material to increase interactions with cells may allow for improved biofunctionality of the print. This may be especially relevant for cases in which cells are temporarily encapsulated within assistive materials and/or the assistive materials are not removed immediately after printing. For example, assistive materials may be designed to provide biochemical and biophysical cues to surrounding or encapsulated cells to aid in their maturation toward the desired phenotype. Exploring biofunctionality of assistive materials to complement the bioink may better promote the ability of prints to mimic not only the form but also the function of native tissues.

For both support baths and sacrificial inks, the removal mechanism is of critical importance to the final print quality and biofunctionality of the construct. In both cases, the removal mechanism must be orthogonal to the bioink itself, that is, it should not impact the bioink material properties or be cross-reactive with other components of the printed structure. Thus, not all bioink compositions will be compatible with every assistive material. For example, if the assistive material is removed through a change in temperature, the bioink's crosslinking mechanism should not also be temperature dependent, otherwise the structural integrity of the print may not be maintained during the removal process. Preventing cross-reactivity becomes even more difficult in multi-material prints, since different bioinks or sacrificial inks may have crosslinking and removal strategies that are not compatible with one another. Moving forward, careful selection of assistive materials along with new developments in bioink crosslinking strategies will be needed so that these processes do not interfere. In addition to orthogonality, the removal mechanism should be as gentle as possible so as to not disrupt cells encapsulated within the bioink or cause a loss of shape fidelity. Therefore, current methods that rely on agitation or physical removal may not be well-suited for prints with very delicate or detailed features. Similarly, methods that involve adding super-physiological levels of ions or large shifts in pH may not be appropriate for cell types that are particularly sensitive to such changes in their environment. Ideally, the removal process should also eliminate all the assistive material, which can be difficult to achieve for materials with a broad sol–gel phase transition. Therefore, removal mechanisms that result in sharp phase transitions under physiological conditions may be preferred. For this reason, gelatin has been a common material for both support baths and sacrificial inks due to its phase change to a solution at 37 °C. For constructs printed within gelatin microgel support baths, the melting time allowed for the gelatin has been between 1 h and 24 h [62]. For gelatin sacrificial ink components within bioinks, the majority of the gelatin (ranging from 57% to 88%) was liberated from the print after 24 h; the amount of gelatin released continued to rise over 15 days yet did not reach complete removal [96]. Incomplete removal of assistive material may influence cells in ways that differ from those of the pure, intended bioink material, and thus should be monitored and quantified. Future work could include optimizing these transitions or making them inducible in response to other external triggers such as specific wavelengths of light, ultrasound, or magnetic/electric fields.

Improvements to 3D bioprinting approaches, including the use of assistive materials, will propel forward the vision of using bioprinted tissue or organ replacements to address the critical shortage of donor organs for patients in need. For example, as discussed previously, use of sacrificial inks to create internal vasculature allows for printing thick tissue-like constructs with high cell survival, which will be essential for full-scale engineered tissues [66, 86, 99]. However, several challenges remain to be considered before 3D bioprinting with assistive materials will be translated into the clinic. In particular, the properties of the bioprinting assistive materials will be subject to more stringent requirements beyond their mechanical characteristics. If animal-derived components are used as the assistive material, then compositional purity will be especially crucial due to risk of prions or transmission of animal retroviruses [120]. Other assistive materials, such as alginate, may induce inflammation if residual amounts remain in the implanted construct [121]. When designing future assistive materials for scaled up and clinically translatable bioprinting applications, synthetic or chemically defined materials may be preferred due to enhanced reproducibility that is necessary for regulation [122, 123]. Finally, maintaining a sterile printing environment will also become increasingly important as the field moves toward creating clinical-grade structures. Currently, at the research scale, bioprinters can be placed within sterile hoods, and ink and support bath materials can be sterilized through UV light exposure or sterile filtration, among other methods [124]. Additional advancements in bioprinter housings to maintain a constant sterile environment may be needed to prevent contamination when printing at larger scales.

In summary, while materials development to advance 3D bioprinting has historically focused on bioinks, materials that play assistive roles are now reinvigorating the field and enabling the next major leap forward. The use of support baths and sacrificial inks improves print fidelity and resolution and broadens the biofabrication window of bioinks to include weaker, less viscous materials that would not otherwise be printable in air. As a result, more complex geometries that better mimic native tissue can be fabricated and scaled up to produce organ-sized constructs. Further adoption and continued design of new assistive materials within the biofabrication field will only increase our ability to create truly biomimetic, functional tissues and organs.

Data availability statement

No new data were created or analyzed in this study.

Acknowledgments

We thank A J Seymour and S Shin for helpful conversations about this manuscript. The authors acknowledge funding support from the National Science Foundation (DMR 2103812, CBET 2033302, DMR 1808415) and the National Institutes of Health (R21 HL138042, R21 NS114549, R01 HL142718, R01 EB027171, R01 HL151997, R01 EB027666). S M H acknowledges funding from a NIH NRSA pre-doctoral fellowship (F31 EY030731) and a Stanford Bio-X Interdisciplinary Graduate Fellowship. L G B acknowledges funding from an NSF Graduate Research Fellowship.

ORCID iDs

Lucia G Brunel https://orcid.org/0000-0003-0327-5635
Sarah M Hull https://orcid.org/0000-0002-3741-654X
Sarah C Heilshorn https://orcid.org/0000-0002-9801-6304

References

[1] Murphy S V and Atala A 2014 3D bioprinting of tissues and organs *Nat. Biotechnol.* **32** 773–85
[2] Groll J *et al* 2016 Biofabrication: reappraising the definition of an evolving field *Biofabrication* **8** 013001
[3] Li J, Chen M, Fan X and Zhou H 2016 Recent advances in bioprinting techniques: approaches, applications and future prospects *J. Transl. Med.* **14** 1–15
[4] Groll J *et al* 2019 A definition of bioinks and their distinction from biomaterial inks *Biofabrication* **11** 013001
[5] Hull S M, Brunel L G and Heilshorn S C 2022 3D bioprinting of cell-laden hydrogels for improved biological functionality *Adv. Mater.* **34** 2103691
[6] Ramesh S, Harrysson O L A, Rao P K, Tamayol A, Cormier D R, Zhang Y and Rivero I V 2021 Extrusion bioprinting: recent progress, challenges, and future opportunities *Bioprinting* **21** e00116
[7] Hunziker E B, Quinn T M and Häuselmann H J 2002 Quantitative structural organization of normal adult human articular cartilage *Osteoarthr. Cartil.* **10** 564–72
[8] Quinn T M, Häuselmann H J, Shintani N and Hunziker E B 2013 Cell and matrix morphology in articular cartilage from adult human knee and ankle joints suggests depth-associated adaptations to biomechanical and anatomical roles *Osteoarthr. Cartil.* **21** 1904–12
[9] Donahue K M, Weisskoff R M, Parmelee D J, Callahan R J, Wilkinson R A, Mandeville J B and Rosen B R 1995 Dynamic Gd-DTPA enhanced MRI measurement of tissue cell volume fraction *Magn. Reson. Med.* **34** 423–32
[10] Peterson H-I 2020 *Tumor Blood Circulation: Angiogenesis, Vascular Morphology and Blood Flow of Experimental and Human Tumors* (Boca Raton, FL: CRC Press)
[11] Everett N B, Simmons B and Lasher E P 1956 Distribution of blood (Fe 59) and plasma (I 131) volumes of rats determined by liquid nitrogen freezing *Circ. Res.* **4** 419–24
[12] Sreter F A and Woo G 1963 Cell water, sodium, and potassium in red and white mammalian muscles *Am. J. Physiol.* **205** 1290–4
[13] Chua C K 2020 Publication trends in 3D bioprinting and 3D food printing *Int. J. Bioprint.* **6** 1–3
[14] Su A and Al'Aref S J 2018 History of 3D printing *3D Print. Appl. Cardiovasc. Med.* (Cambridge, MA: Academic Press) pp 1–10
[15] Hull C W 1984 Apparatus for production of three dimensional objects by stereolithography
[16] Deckard C R 1986 Apparatus for producing parts by selective sintering
[17] Crump S S 1989 Modeling apparatus for three-dimensional objects
[18] Gu Z, Fu J, Lin H and He Y 2020 Development of 3D bioprinting: from printing methods to biomedical applications *Asian J. Pharm. Sci.* **15** 529–57
[19] Boland T, Wilson W and Xu T 2003 Ink-jet printing of viable cells
[20] Forgacs G, Jakab K, Neagu A and Mironov V 2004 Self-assembling cell aggregates and methods of making engineered tissue using the same
[21] Schwab A, Levato R, D'Este M, Piluso S, Eglin D and Malda J 2020 Printability and shape fidelity of bioinks in 3D bioprinting *Chem. Rev.* **120** 11028–55
[22] Malda J, Visser J, Melchels F P, Jüngst T, Hennink W E, Dhert W J A, Groll J and Hutmacher D W 2013 25th anniversary article: engineering hydrogels for biofabrication *Adv. Mater.* **25** 5011–28
[23] Shiwarski D J, Hudson A R, Tashman J W and Feinberg A W 2021 Emergence of FRESH 3D printing as a platform for advanced tissue biofabrication *APL Bioeng.* **5** 10904
[24] Cho D-W 2019 *Biofabrication and 3D Tissue Modeling* (London: Royal Society of Chemistry)
[25] Jakab K, Damon B, Neagu A, Kachurin A and Forgacs G 2006 Three-dimensional tissue constructs built by bioprinting *Biorheology* **43** 509–13
[26] Highley C B, Rodell C B and Burdick J A 2015 Direct 3D printing of shear-thinning hydrogels into self-healing hydrogels *Adv. Mater.* **27** 5075–9
[27] Bhattacharjee T, Zehnder S M, Rowe K G, Jain S, Nixon R M, Sawyer W G and Angelini T E 2015 Writing in the granular gel medium *Sci. Adv.* **1** e1500655
[28] Hinton T J, Jallerat Q, Palchesko R N, Park J H, Grodzicki M S, Shue H-J, Ramadan M H, Hudson A R and Feinberg A W 2015 Three-dimensional printing of complex biological structures by freeform reversible embedding of suspended hydrogels *Sci. Adv.* **1** e1500758
[29] Cooke M E and Rosenzweig D H 2021 The rheology of direct and suspended extrusion bioprinting *APL Bioeng.* **5** 011502
[30] Xie Z-T, Kang D-H and Matsusaki M 2021 Resolution of 3D bioprinting inside bulk gel and granular gel baths *Soft Matter* **17** 8769–85

[31] Loh Q L and Choong C 2013 Three-dimensional scaffolds for tissue engineering applications: role of porosity and pore size *Tissue Eng.* B **19** 485
[32] Therriault D, White S R and Lewis J A 2003 Chaotic mixing in three-dimensional microvascular networks fabricated by direct-write assembly *Nat. Mater.* **2** 265–71
[33] Wu W, Deconinck A and Lewis J A 2011 Omnidirectional printing of 3D microvascular networks *Adv. Mater.* **23** H178–83
[34] Miller J S *et al* 2012 Rapid casting of patterned vascular networks for perfusable engineered three-dimensional tissues *Nat. Mater.* **11** 768–74
[35] Kolesky D B, Truby R L, Gladman A S, Busbee T A, Homan K A and Lewis J A 2014 3D bioprinting of vascularized, heterogeneous cell-laden tissue constructs *Adv. Mater.* **26** 3124–30
[36] Chopin-Doroteo M, Mandujano-Tinoco E A and Krötzsch E 2021 Tailoring of the rheological properties of bioinks to improve bioprinting and bioassembly for tissue replacement *Biochim. Biophys. Acta* **1865** 129782
[37] Seymour A J, Shin S and Heilshorn S C 2021 3D printing of microgel scaffolds with tunable void fraction to promote cell infiltration *Adv. Healthcare Mater.* **10** 2100644
[38] Ying G-L, Jiang N, Mahar S, Yin Y-X, Chai R-R, Cao X, Yang J-Z, Miri A K, Hassan S and Zhang Y S 2018 Aqueous two-phase emulsion bioink-enabled 3D bioprinting of porous hydrogels *Adv. Mater.* **30** 1805460
[39] Ying G, Jiang N, Parra-Cantu C, Tang G, Zhang J, Wang H, Chen S, Huang N P, Xie J and Zhang Y S 2020 Bioprinted injectable hierarchically porous gelatin methacryloyl hydrogel constructs with shape-memory properties *Adv. Funct. Mater.* **30** 2003740
[40] Levato R, Jungst T, Scheuring R G, Blunk T, Groll J and Malda J 2020 From shape to function: the next step in bioprinting *Adv. Mater.* **32** 1906423
[41] Sun W *et al* 2020 The bioprinting roadmap *Biofabrication* **12** 022002
[42] Baker B M and Chen C S 2012 Deconstructing the third dimension: how 3D culture microenvironments alter cellular cues *J. Cell Sci.* **125** 3015–24
[43] Engler A J, Sen S, Sweeney H L and Discher D E 2006 Matrix elasticity directs stem cell lineage specification *Cell* **126** 677–89
[44] Lo C-M, Wang H-B, Dembo M and Wang Y-L 2000 Cell movement is guided by the rigidity of the substrate *Biophys. J.* **79** 144–52
[45] Yeung T, Georges P C, Flanagan L A, Marg B, Ortiz M, Funaki M, Zahir N, Ming W, Weaver V and Janmey P A 2005 Effects of substrate stiffness on cell morphology, cytoskeletal structure, and adhesion *Cell Motil. Cytoskeleton* **60** 24–34
[46] Hadjipanayi E, Mudera V and Brown R A 2009 Close dependence of fibroblast proliferation on collagen scaffold matrix stiffness *J. Tissue Eng. Regen. Med.* **3** 77–84
[47] Nelson A Z, Kundukad B, Wong W K, Khan S A and Doyle P S 2020 Embedded droplet printing in yield-stress fluids *Proc. Natl Acad. Sci.* **117** 5671–9
[48] Hull S M, Lindsay C D, Brunel L G, Shiwarski D J, Tashman J W, Roth J G, Myung D, Feinberg A W and Heilshorn S C 2020 3D bioprinting using UNIversal Orthogonal Network (UNION) bioinks *Adv. Funct. Mater.* **31** 2007983
[49] Basu A, Saha A, Goodman C, Shafranek R T and Nelson A 2017 Catalytically initiated gel-in-gel printing of composite hydrogels *ACS Appl. Mater. Interfaces* **9** 40898–904
[50] O'Bryan C S, Kabb C P, Sumerlin B S and Angelini T E 2019 Jammed polyelectrolyte microgels for 3D cell culture applications: rheological behavior with added salts *ACS Appl. BioMater.* **2** 1509–17
[51] O'Bryan C S, Bhattacharjee T, Hart S, Kabb C P, Schulze K D, Chilakala I, Sumerlin B S, Sawyer W G and Angelini T E 2017 Self-assembled micro-organogels for 3D printing silicone structures *Sci. Adv.* **3** e1602800
[52] LeBlanc K J, Niemi S R, Bennett A I, Harris K L, Schulze K D, Sawyer W G, Taylor C and Angelini T E 2016 Stability of high speed 3D printing in liquid-like solids *ACS Biomater. Sci. Eng.* **2** 1796–9
[53] Grosskopf A K, Truby R L, Kim H, Perazzo A, Lewis J A and Stone H A 2018 Viscoplastic matrix materials for embedded 3D printing *ACS Appl. Mater. Interfaces* **10** 23353–61
[54] Jin Y, Chai W and Huang Y 2017 Printability study of hydrogel solution extrusion in nanoclay yield-stress bath during printing-then-gelation biofabrication *Mater. Sci. Eng.* C **80** 313–25
[55] Muth J T, Vogt D M, Truby R L, Mengüç Y, Kolesky D B, Wood R J and Lewis J A 2014 Embedded 3D printing of strain sensors within highly stretchable elastomers *Adv. Mater.* **26** 6307–12
[56] Guimarães C F, Gasperini L, Marques A P and Reis R L 2020 The stiffness of living tissues and its implications for tissue engineering *Nat. Rev. Mater.* **5** 351–70
[57] Butcher D T, Alliston T and Weaver V M 2009 A tense situation: forcing tumour progression *Nat. Rev. Cancer* **9** 108–22
[58] Iskratsch T, Wolfenson H and Sheetz M P 2014 Appreciating force and shape—the rise of mechanotransduction in cell biology *Nat. Rev. Mol. Cell Biol.* **15** 825–33
[59] Townsend J M, Beck E C, Gehrke S H, Berkland C J and Detamore M S 2019 Flow behavior prior to crosslinking: the need for precursor rheology for placement of hydrogels in medical applications and for 3D bioprinting *Prog. Polym. Sci.* **91** 126–40
[60] Nelson A Z, Schweizer K S, Rauzan B M, Nuzzo R G, Vermant J and Ewoldt R H 2019 Designing and transforming yield-stress fluids *Curr. Opin. Solid State Mater. Sci.* **23** 100758
[61] Jeon O, Bin L Y, Jeong H, Lee S J, Wells D and Alsberg E 2019 Individual cell-only bioink and photocurable supporting medium for 3D printing and generation of engineered tissues with complex geometries *Mater. Horiz.* **6** 1625–31
[62] Lee A, Hudson A R, Shiwarski D J, Tashman J W, Hinton T J, Yerneni S, Bliley J M, Campbell P G and Feinberg A W 2019 3D bioprinting of collagen to rebuild components of the human heart *Science* **365** 482–7
[63] Morley C D *et al* 2019 Quantitative characterization of 3D bioprinted structural elements under cell generated forces *Nat. Commun.* **10** 1–9
[64] Bhattacharjee T, Zehnder S M, Rowe K G, Jain S, Nixon R M, Sawyer W G and Angelini T E 2015 Writing in the granular gel medium *Sci. Adv.* **1** e150065
[65] O'Bryan C S, Bhattacharjee T, Marshall S L, Gregory Sawyer W and Angelini T E 2018 Commercially available microgels for 3D bioprinting *Bioprinting* **11** e00037
[66] Skylar-Scott M A, Uzel S G M, Nam L L, Ahrens J H, Truby R L, Damaraju S and Lewis J A 2019 Biomanufacturing of organ-specific tissues with high cellular density and embedded vascular channels *Sci. Adv.* **5** eaaw2459
[67] Compaan A M, Song K and Huang Y 2019 Gellan fluid gel as a versatile support bath material for fluid extrusion bioprinting *ACS Appl. Mater. Interfaces* **11** 5714–26
[68] Song K H, Highley C B, Rouff A and Burdick J A 2018 Complex 3D-printed microchannels within cell-degradable hydrogels *Adv. Funct. Mater.* **28** 1801331
[69] Jin Y, Compaan A, Bhattacharjee T and Huang Y 2016 Granular gel support-enabled extrusion of three-dimensional alginate and cellular structures *Biofabrication* **8** 025016
[70] Noor N, Shapira A, Edri R, Gal I, Wertheim L and Dvir T 2019 3D printing of personalized thick and perfusable cardiac patches and hearts *Adv. Sci.* **6** 1900344
[71] Moxon S R, Cooke M E, Cox S C, Snow M, Jeys L, Jones S W, Smith A M and Grover L M 2017 Suspended

manufacture of biological structures *Adv. Mater.* **29** 1605594
[72] Jin Y, Compaan A, Chai W and Huang Y 2017 Functional nanoclay suspension for printing-then-solidification of liquid materials *ACS Appl. Mater. Interfaces* **9** 20057–66
[73] Shin S and Hyun J 2017 Matrix-assisted three-dimensional printing of cellulose nanofibers for paper microfluidics *ACS Appl. Mater. Interfaces* **9** 26438–46
[74] Brassard J A, Nikolaev M, Hübscher T, Hofer M and Lutolf M P 2021 Recapitulating macro-scale tissue self-organization through organoid bioprinting *Nat. Mater.* **20** 22–29
[75] Lawlor K T *et al* 2021 Cellular extrusion bioprinting improves kidney organoid reproducibility and conformation *Nat. Mater.* **20** 260–71
[76] Daly A C, Davidson M D and Burdick J A 2021 3D bioprinting of high cell-density heterogeneous tissue models through spheroid fusion within self-healing hydrogels *Nat. Commun.* **12** 753
[77] Mirdamadi E, Tashman J W, Shiwarski D J, Palchesko R N and Feinberg A W 2020 FRESH 3D bioprinting a full-size model of the human heart *ACS Biomater. Sci. Eng.* **6** 6453–9
[78] Miri A K, Mirzaee I, Hassan S, Mesbah Oskui S, Nieto D, Khademhosseini A and Zhang Y S 2019 Effective bioprinting resolution in tissue model fabrication *Lab Chip* **19** 2019–37
[79] Lee J M, Ng W L and Yeong W Y 2019 Resolution and shape in bioprinting: strategizing towards complex tissue and organ printing *Appl. Phys. Rev.* **6** 11307
[80] Tashman J W, Shiwarski D J, Ruesch A, Lanni F, Kainerstorfer J M and Feinberg A W 2021 *In situ* volumetric imaging and analysis of FRESH 3D bioprinted constructs using optical coherence tomography *bioRxiv* https://doi.org/10.1101/2021.06.30.450389
[81] Ning L, Mehta R, Cao C, Theus A, Tomov M, Zhu N, Weeks E R, Bauser-Heaton H and Serpooshan V 2020 Embedded 3D bioprinting of gelatin methacryloyl-based constructs with highly tunable structural fidelity *ACS Appl. Mater. Interfaces* **12** 44563–77
[82] Lee K Y, Rowley J A, Eiselt P, Moy E M, Bouhadir K H and Mooney D J 2000 Controlling mechanical and swelling properties of alginate hydrogels independently by cross-linker type and cross-linking density *Macromolecules* **33** 4291–4
[83] McCormack A, Highley C B, Leslie N R and Melchels F P W 2020 3D printing in suspension baths: keeping the promises of bioprinting afloat *Trends Biotechnol.* **38** 584–93
[84] Zhang Y, Kumar P, Lv S, Xiong D, Zhao H, Cai Z and Zhao X 2021 Recent advances in 3D bioprinting of vascularized tissues *Mater. Des.* **199** 109398
[85] Seymour A J, Westerfield A D, Cornelius V C, Skylar-Scott M A and Heilshorn S C 2022 Bioprinted microvasculature: progressing from structure to function *Biofabrication* **14** 022002
[86] Kolesky D B, Homan K A, Skylar-Scott M A and Lewis J A 2016 Three-dimensional bioprinting of thick vascularized tissues *Proc. Natl Acad. Sci.* **113** 3179 LP—3184
[87] Visser J, Peters B, Burger T J, Boomstra J, Dhert W J A, Melchels F P W and Malda J 2013 Biofabrication of multi-material anatomically shaped tissue constructs *Biofabrication* **5** 035007
[88] Norotte C, Marga F S, Niklason L E and Forgacs G 2009 Scaffold-free vascular tissue engineering using bioprinting *Biomaterials* **30** 5910–7
[89] Bertassoni L E *et al* 2014 Direct-write bioprinting of cell-laden methacrylated gelatin hydrogels *Biofabrication* **6** 24105
[90] Bertassoni L E *et al* 2014 Hydrogel bioprinted microchannel networks for vascularization of tissue engineering constructs *Lab Chip* **14** 2202–11
[91] Wang X Y, Jin Z H, Gan B W, Lv S W, Xie M and Huang W H 2014 Engineering interconnected 3D vascular networks in hydrogels using molded sodium alginate lattice as the sacrificial template *Lab Chip* **14** 2709–16
[92] Hammer J, Han L-H, Tong X and Yang F 2014 A facile method to fabricate hydrogels with microchannel-like porosity for tissue engineering *Tissue Eng.* C **20** 169–76
[93] Gu Z T, Wang H, Li L, Liu Y S, Deng X B, Huo S F, Yuan F F, Liu Z F, Tong H S and Su L 2014 Heat stress induces apoptosis through transcription-independent p53-mediated mitochondrial pathways in human umbilical vein endothelial cell *Sci. Rep.* **4** 4469
[94] Aydin L, Kucuk S and Kenar H 2020 A universal self-eroding sacrificial bioink that enables bioprinting at room temperature *Polym. Adv. Technol.* **31** 1634–47
[95] Ozbolat V, Dey M, Ayan B and Ozbolat I T 2019 Extrusion-based printing of sacrificial Carbopol ink for fabrication of microfluidic devices *Biofabrication* **11** 034101
[96] Ouyang L, Armstrong J P K, Lin Y, Wojciechowski J P, Lee-Reeves C, Hachim D, Zhou K, Burdick J A and Stevens M M 2020 Expanding and optimizing 3D bioprinting capabilities using complementary network bioinks *Sci. Adv.* **6** 1–14
[97] Lee W, Lee V, Polio S, Keegan P, Lee J H, Fischer K, Park J K and Yoo S S 2010 On-demand three-dimensional freeform fabrication of multi-layered hydrogel scaffold with fluidic channels *Biotechnol. Bioeng.* **105** 1178–86
[98] Lee V K, Kim D Y, Ngo H, Lee Y, Seo L, Yoo S S, Vincent P A and Dai G 2014 Creating perfused functional vascular channels using 3D bio-printing technology *Biomaterials* **35** 8092–102
[99] Pimentel R C, Ko S K, Caviglia C, Wolff A, Emnéus J, Keller S S and Dufva M 2018 Three-dimensional fabrication of thick and densely populated soft constructs with complex and actively perfused channel network *Acta Biomater.* **65** 174–84
[100] Hamidi A and Tadesse Y 2020 3D printing of very soft elastomer and sacrificial carbohydrate glass/elastomer structures for robotic applications *Mater. Des.* **187** 108324
[101] Miller J S *et al* 2012 Rapid casting of patterned vascular networks for perfusable engineered 3D tissues *Nat. Mater.* **11** 768
[102] Betts J G, Young K A, Wise J A, Johnson E, Poe B, Kruse D H, Korol O, Johnson J E, Womble M and DeSaix P 2013 *Anatomy and Physiology* (OpenStax)
[103] Na K, Shin S, Lee H, Shin D, Baek J, Kwak H, Park M, Shin J and Hyun J 2018 Effect of solution viscosity on retardation of cell sedimentation in DLP 3D printing of gelatin methacrylate/silk fibroin bioink *J. Ind. Eng. Chem.* **61** 340–7
[104] Dubbin K, Tabet A and Heilshorn S C 2017 Quantitative criteria to benchmark new and existing bio-inks for cell compatibility *Biofabrication* **9** 044102
[105] Dubbin K, Hori Y, Lewis K K and Heilshorn S C 2016 Dual-stage crosslinking of a gel-phase bioink improves cell viability and homogeneity for 3D bioprinting *Adv. Healthcare Mater.* **5** 2488–92
[106] Ouyang L, Highley C B, Rodell C B, Sun W and Burdick J A 2016 3D printing of shear-thinning hyaluronic acid hydrogels with secondary cross-linking *ACS Biomater. Sci. Eng.* **2** 1743–51
[107] Shin S, Park S, Park M, Jeong E, Na K, Youn H J and Hyun J 2017 Cellulose nanofibers for the enhancement of printability of low viscosity gelatin derivatives *BioResources* **12** 2941–54
[108] Hagel V, Haraszti T and Boehm H 2013 Diffusion and interaction in PEG-DA hydrogels *Biointerphases* **8** 1–9
[109] Lee K, Chen Y, Li X, Wang Y, Kawazoe N, Yang Y and Chen G 2019 Solution viscosity regulates chondrocyte proliferation and phenotype during 3D culture *J. Mater. Chem.* B **7** 7713
[110] Zaman M H, Trapani L M, Siemeski A, MacKellar D, Gong H, Kamm R D, Wells A, Lauffenburger D A and Matsudaira P 2006 Migration of tumor cells in 3D matrices is governed by matrix stiffness along with cell-matrix

adhesion and proteolysis *Proc. Natl Acad. Sci. USA* **103** 10889–94
[111] Compaan A M, Christensen K and Huang Y 2017 Inkjet bioprinting of 3D silk fibroin cellular constructs using sacrificial alginate *ACS Biomater. Sci. Eng.* **3** 1519–26
[112] Johnson T, Bahrampourian R, Patel A and Mequanint K 2010 Fabrication of highly porous tissue-engineering scaffolds using selective spherical porogens *Biomed. Mater. Eng.* **20** 107–18
[113] Tran R T, Naseri E, Kolasnikov A, Bai X and Yang J 2011 A new generation of sodium chloride porogen for tissue engineering *Biotechnol. Appl. Biochem.* **58** 335–44
[114] Mouser V H M, Melchels F P W, Visser J, Dhert W J A, Gawlitta D and Malda J 2016 Yield stress determines bioprintability of hydrogels based on gelatin-methacryloyl and gellan gum for cartilage bioprinting *Biofabrication* **8** 035003
[115] Schuurman W, Levett P A, Pot M W, van Weeren P R, Dhert W J A, Hutmacher D W, Melchels F P W, Klein T J and Malda J 2013 Gelatin-methacrylamide hydrogels as potential biomaterials for fabrication of tissue-engineered cartilage constructs *Macromol. Biosci.* **13** 551–61
[116] Nair K, Gandhi M, Khalil S, Yan K C, Marcolongo M, Barbee K and Sun W 2009 Characterization of cell viability during bioprinting processes *Biotechnol. J.* **4** 1168–77
[117] Aguado B A, Mulyasasmita W, Su J, Lampe K J and Heilshorn S C 2012 Improving viability of stem cells during syringe needle flow through the design of hydrogel cell carriers *Tissue Eng.* A **18** 806–15
[118] Olsen B D, Kornfield J A and Tirrell D A 2010 Yielding behavior in injectable hydrogels from telechelic proteins *Macromolecules* **43** 9094–9
[119] Gao T, Gillispie G J, Copus J S, Kumar A P R, Seol Y-J, Atala A, Yoo J J and Lee S J 2018 Optimization of gelatin-alginate composite bioink printability using rheological parameters: a systematic approach *Biofabrication* **10** 034106
[120] Taylor P M, Cass A E G and Yacoub M H 2006 Extracellular matrix scaffolds for tissue engineering heart valves *Prog. Pediatr. Cardiol.* **21** 219–25
[121] Yang D and Jones K S 2009 Effect of alginate on innate immune activation of macrophages *J. Biomed. Mater. Res.* A **90A** 411–8
[122] Kohane D S and Langer R 2008 Polymeric biomaterials in tissue engineering *Pediatr. Res.* **63** 487–91
[123] Sengupta D and Heilshorn S C 2010 Protein-engineered biomaterials: highly tunable tissue engineering Scaffolds *Tissue Eng.* B **16** 285–93
[124] Galante R, Pinto T J A, Colaço R and Serro A P 2018 Sterilization of hydrogels for biomedical applications: a review *J. Biomed. Mater. Res.* B **106** 2472–92